

Stevin report 25.6.90.11/A1/12.05

TNO-IBBC report BI-90-093/63.5.3820

THE FATIGUE BEHAVIOUR OF AXIALLY LOADED T-JOINTS BETWEEN RECTANGULAR  
HOLLOW SECTIONS UNDER RANDOM LOADING

by A. Verheul  
J. Wardenier  
J. de Back

October 1990

## CONTENTS

page

### PREFACE

### LIST OF SYMBOLS

1. Introduction	1
2. Test specimen	1
3. Material properties	2
4. Load spectrum	2
5. Test rig and testing procedure	3
6. Measurements	3
7. Test results	5
7.1 Strain range determination	5
7.1.1 Strain range extrapolation to the weld toe	5
7.1.2 Strain concentration factor (SNCF)	6
7.2 Fatigue test	6
7.2.1 Strain distribution	7
7.2.2 Mode of failure	8
7.2.3 $S_r$ -N diagrams	8
8. Summary and conclusion	10
9. References	12

3 tables

21 figures

The figures 22 to 53 are given in appendix 1

## PREFACE

Within the framework of the research programme "The fatigue behaviour of axially loaded T-joints between rectangular hollow sections " eight fatigue tests under random loading were carried out.

The aim of this research programme is to establish evidence for the fatigue strength of joints in square hollow sections under random loading.

The results are compared with the high cycle fatigue results of the ECSC research programme [1] and the low cycle fatigue results of the Cidect research programme [2] and various recommended curves.

The eight T-joints were tested under a linear spectrum with  $P = F_{r \min} / F_{r \max} = 1/3$  or  $2/3$  ( $F_{r \min}$  and  $F_{r \max}$  is the minimum resp. maximum loadrange in the spectrum). The chords had the dimension  $200 \times 200 \times 12.5$  whereas the braces were either  $140 \times 140 \times 8$  or  $140 \times 140 \times 5$ . Consequently the ratio  $P$  and the thickness ratio  $r$  were varied. The different thickness ratios resulted in different failure modes i.e. chord or brace failure. The results are presented based on the hot spot strain range using quadratic extrapolation of the geometrical strain to the weld toe but are also given based on the nominal stress range. Furthermore strain distributions in the specimens are presented.

## ACKNOWLEDGEMENTS

The donation by "Van Leeuwen Buizen" - Zwijndrecht and Oving-Diepenveen-struyken" b.v. - Barendrecht of the hollow sections used in this programme is appreciated.

## LIST OF SYMBOLS

$A_0$	: cross sectional area of chord
$A_1$	: cross sectional area of brace
$F$	: axial load
$F_{r_i}$	: axial load range $F_{\max} - F_{\min}$
$F_{r_{eq}}$	: equivalent load range
$N$	: number of cycles
$N_f$	: number of cycles to failure
$N_i$	: number of cycles to initiation of cracks
$P$	: spectrum ratio $\frac{F_{r_{\min}}}{F_{r_{\max}}}$
$S_r$	: stress range $\sigma_{\max} - \sigma_{\min}$
$S_{r_{ab}}$	: nominal stress range in the brace
$S_{r_{h.s}}$	: hot spot stress range
SCF	: stress concentration factor, $= \sigma/\sigma_{ab}$
SNCF	: strain concentration factor, $= \epsilon/\epsilon_{ab}$
$a$	: throat thickness of the fillet welds
$a_h$	: projected length of the weld along chord face
$a_v$	: projected length of the weld along brace axis
$b_0$	: external width of chord member
$b_1$	: external width of brace member
$n_i$	: number of load cycles with load range $F_{r_i}$
$r_{0_0}$	: measured projected length of the curved corners of the chord (see table 3)
$r_{1_0}$	: measured projected length of the curved corners of the brace (see table 3)
$t_0$	: wall thickness of the chord member
$t_1$	: wall thickness of the chord member
$t_{0_4}$	: measured wall thickness in corners of chord members
$t_{1_3}$	: measured wall thickness in corners of brace members
$\beta$	: brace to chord width ratio
$2\gamma$	: with to wall thickness ratio of the chord $b_0/t_0$
$\epsilon$	: strain
$\epsilon_{ab}$	: axial strain in the brace
$\epsilon_0$	: ultimate elongation of the chord member

$\epsilon_1$  : ultimate elongation of the brace member  
 $\epsilon_r$  : strain range  
 $\epsilon_{r_{ab}}$  : nominal strain range in the brace  
 $\epsilon_{r_{hs}}$  : hot spot strain range  
 $f_{y0}$  : yield stress of the chord member  
 $f_{y1}$  : yield stress of the brace member  
 $f_{u0}$  : ultimate stress of the chord member  
 $f_{u1}$  : ultimate stress of the brace member  
 $\sigma_{max.}$  : maximum stress  
 $\sigma_{min.}$  : minimum stress  
 $\tau$  : wall thickness ratio between brace and chord member  $t_1/t_0$

## 1. INTRODUCTION

Most of the design recommendations for fatigue are based on constant amplitude fatigue tests.

This research programme "The fatigue behaviour under random loading of axially loaded T-joints between rectangular hollow sections" covers an experimental investigation on the fatigue behaviour under random loading of 8 rectangular hollow section T-joints.

The results will be compared with the results of previous high cycle and low cycle constant amplitude fatigue tests [1,2] therefore the same dimensions for the specimens are used. The results will also be compared with various existing curves.

The work has been carried out at the Delft University of Technology.

## 2. TEST SPECIMENS

A review of the T-joint specimens with their identification number is given in table 1. The configuration of these specimens is given in the Figs. 1,3 and 4. The actual dimensions are recorded in table 3.

With respect to the geometry following nominal dimensions are used for the test specimens:

- four specimens with chord 200\*200\*12.5 and brace 140\*140\*5
- four specimens with chord 200\*200\*12.5 and brace 140\*140\*8

The eight T-joints for this experimental investigation have non dimensional parameters  $2\gamma = 16$  and  $\beta = 0.7$ , and a thickness ratio  $r = 0.4$  or  $0.64$ .

All test specimens are welded with rutile electrodes (trade name OMNIA) in accordance with standards NEN 1062, ERA 112, NBN F-31-001, E 432R, ASME SFA-5.1, E 6013, DIN 1933, E 43 22 R(C)3, BS 639 and E 43 22R.

The specimens with a wall thickness of the brace of 5 mm are welded with fillet welds (3 layers). The specimens with a wall thickness of the brace of 8 mm are welded with butt welds (4 layers).

The specimens were welded in a position with the chord horizontal and the brace vertical. Plates were welded to the ends of the chord and brace for mounting into the test rig.

### 3. MATERIAL PROPERTIES

The rectangular hollow sections are hot finished with a steel grade Fe 430D for the sections 200\*200\*12.5 and Fe 430C for the sections 140\*140\*5 and 140\*140\*8, according to the Euronorm 25-72.

The measured dimensions and the actual mechanical properties of the hollow sections are recorded in table 3. The actual wall thicknesses are given in average values, measured in the middle of the walls. The measured thickness in the corner is greater, with the wall thickness varying along the width of the sections. The measured outer corner radii of the sections 140\*140\*5, 140\*140\*8 and 200\*200\*12.5 are respectively 14%, 10% and 40% smaller than the nominal values.

The yield stresses  $f_y$  of all the sections were determined with stub column tests (see table 3). The stub columns had lengths of  $2.5b$ . For a better visual indication of yielding the stub columns were whitewashed. The ultimate stress and the permanent elongation were determined with tensile tests (dp 5), carried out in accordance with Euronorm 2-57 "tensile tests for steel". The tensile coupons were taken from the middle of a face of the hollow sections in the longitudinal direction.

### 4. LOAD SPECTRUM

The eight fatigue tests were carried out under random loading applying a load spectrum with  $P = 1/3$  or  $2/3$  and a spectrum length of  $5 \cdot 10^4$  (see fig. 5 and 6). The minimum load  $F_{\min}$  was 2 kN.

This spectrum was repeated till the end of the test.

Fig 5. shows the loading spectra with the specimens numbers.

The load range has been given on the Y-axis on a linear scale whereas the number of cycles has been given on the X-axis on a logarithmic scale.



For testing the load ratio  $P$  has been divided into blocks of equal steps as shown in fig. 6. However the spectrum for  $P = 1/3$  has been divided into twice as much loading steps as for  $P = 2/3$  for having the same deviation of the spectrum curve.

## 5. TEST RIG AND TESTING PROCEDURE

Figure 2 shows the test rig for the T-joint specimens. The dynamic axial load was applied by a servo hydraulic actuator of 1600 kN. The specimen was mounted into the test rig in such a way that possible moments in plane could be adjusted.

To avoid secondary effects all supports in the test rig are hinges. The end supports of the chord were realized by a ball joint at one end and a roller bearing at the other end. The number of cycles and the measured data to it were recorded on a control unit.

Before starting the fatigue test a static load equal to the equivalent dynamic loadrange of the spectrum was applied. After 10 cycles to this load level no yielding occurred and the first strain measurements were carried out.

During fatigue testing the number of cycles at crack initiation and complete failure of the joint were determined.

The load spectrum used has a sinusoidal wave form with a frequency of 1.5 Hz.

The load spectrum was built up in blocks with the number of cycles cumulatively and a load range ratio of  $P = F_{r \text{ min}} / F_{r \text{ max}} = 1/3$  or  $2/3$  (see fig 5 and 6). However, the load cycles were within this spectrum randomly applied. During the testing the load levels were controlled by a loading control unit which was connected to the hydraulic system of the jack. During the fatigue testing the load levels were maintained irrespective of the deformation of the joint.

## 6. MEASUREMENTS

During testing the axial load on the brace was measured with a dynamometer. To determine the nominal strain range the brace of each specimen was provided with strain gauges in a cross section. A second

cross section was provided with strain gauges to determine possible moments due to eccentricities. The distances to the end plate and the chord face were chosen in such a way that the "end effects" are expected to be neglectable. All specimens were provided with strain gauges and strain chains at the corner locations of the chord and brace at the intersection. The strain gauges and strain chain locations for the various specimens are given in the figures 7 to 8.

The previous tests on T-joints [1,2] showed that the maximum hot spot strain range occurred at the location A for the brace and at location C for the chord (see fig. 9). For the specimens with a brace thickness  $t_1 = 5$  mm the crack generally started at location A and exceptionally at location C, however, for the specimens with  $t_1 = 8$  mm the crack always started in the chord at location C. Consequently for the specimens with  $t_1 = 5$  mm the locations A and C are provided with strain gauges whereas for the specimens with  $t_1 = 8$  mm only location C has been provided with strain gauges.

Each load range and strain range was recorded by a computer and the number of cycles in each block was counted. The load spectrum of each specimen determined from the measurements is given in appendix 1 (fig 22 to 29). In these figures the Y-axis gives the measured load ranges, whereas on the X-axis the number of cycles belonging to it are given cumulatively.

The equivalent load range was determined by using the Miner rule:

$$F_{req} = \sqrt[m]{\frac{\sum n_i}{\sum \frac{n_i}{(F_{r_i})^m}}}$$

In this formula the exponent  $m$  is based on curve D which represents the mean results of the previous high cycle constant amplitude fatigue tests [1]. For the failed members with a wall thickness of 12.5 mm,  $m = -3.389$  whereas for the failed members with a wall thickness of 5 mm,  $m = -3.526$

Since at the start of the fatigue test the value of the ratio  $F_r / \epsilon_r$  was constant, changes of this value during fatigue testing gave an

indication of crack initiation. After visually observation of the first cracks the crack growth was followed and recorded.

## 7. TEST RESULTS

### 7.1 Strain range determination

The nominal strain range in the brace was determined by the average value of the strain gauge measurements in the cross section B-B (see fig. 7 to 8). The hot spot strain ranges in the joint were measured at various locations in the joint. All strain range measurements were carried out dynamically. The strain measurements after the initial 10 cycles were used as bases for the analyses.

#### 7.1.1 Strain range extrapolation to the weld toe

The actual strain range at the weld toe is affected by:

- Type of loading (axial, bending in plane or out of plane)
- Type of joint (T, X, K, etc).
- Overall geometry of a particular type of joints ( $\alpha$ ,  $\beta$ ,  $\gamma$ ,  $\tau$ ,).
- Local geometry (shape and stiffness of the weld, weld toe radius).

In the current offshore design the local geometry of the weld and weld toe is excluded for the determination of the geometrical hot spot strain. All other influencing factors such as type of loading, type of joint and overall geometry are taken into account for the fatigue design and the analysis. This means that only the very local effects at the weld toe (radius, angle) are excluded.

To avoid the local effects of the weld toe the first extrapolation point is taken at  $0.4t_1$  or  $0.4t_0$  but not smaller than 4 mm

(see fig. 10) which is in line with current experience with joints of circular hollow sections [4]. In earlier ECSC offshore programmes a linear extrapolation to the weld toe was used. Later work on overlap joints and joints with large  $\beta$  ratios showed that a non linear extrapolation may probably be more appropriate. This was confirmed by

the programme on rectangular hollow sections [1]. Therefore in this research programme the quadratic extrapolation method is used (see fig. 10).

#### 7.1.2 Strain concentration factor (SNCF)

For comparison with the test results and the numerical results [3] the hot spot strain ranges are used to determine the hot spot strain concentration factors (see fig. 11 to 15). These are defined as follows:

$$\text{SNCF} = \frac{\text{extrapolated hot spot strain to the weld toe}}{\text{nominal strain in the brace}}$$

The SNCF's for the chord and brace are recorded in table 2.

#### 7.2 Fatigue test results

The fatigue test results are summarized in table 2, which shows:

- test number,
- chord and brace dimensions (nominal),
- the spectrum load ratio  $P = F_{r \min} / F_{r \max} = 1/3$  or  $2/3$
- maximum and minimum and equivalent load range, nominal stress range and strain range,
- maximum, minimum and equivalent hot spot strain range in chord and brace, based on the crack location
- the maximum strain concentration factor in chord and brace (location A and C), at the crack location.
- the number of cycles to crack initiation  $N_i$  and the number of cycles to failure  $N_f$ ,
- mode of failure (crack location)

The results are analyzed using quadratic extrapolation based on crack location

The equivalent load ranges and strain ranges were determined by using the Miner rule (chap. 6.) and based on curve D which represents the mean results of the previous high cycle constant amplitude fatigue tests [1].

### 7.2.1 Strain distribution

All the results of the dynamic strain measurements (equivalent) for the locations given in the figures 7 to 8 are given in appendix 1 (figs 30 to 53). The measured strain ranges at symmetrical locations of the joint are indicated with symbols in the same figure and are plotted on the actual distance from the weld toe. The measured strain ranges are converted into strain concentration factors ( $SNCF = \epsilon_r / \epsilon_{rab}$ ) and given in appendix 1. These figures show the extrapolation curve of the SNCF's of the corner where the crack started first.

Figures 11 to 15 show the strain distribution in the various specimens. These figures show the background information of table 2. For the cracked member SNCF's have been given at the corner where the crack started first. However, for the other member the maximum measured SNCF has been given to.

Figure 14 shows the mean extrapolation lines A (based on crack location) for the specimens tested with  $P = 1/3$  resp.  $2/3$ . The large difference between the two extrapolated values is due to specimen T27 which had a large scatter of the extrapolated values of the four corners (see fig. 39).

Figure 15 shows the mean extrapolation lines C (based on crack location) for the specimens tested with  $P = 1/3$  resp.  $2/3$ .

Furthermore it is clearly shown that the SNCF in the brace (line A) is higher than in the chord (line C). For the specimens with  $r = 0.4$  this difference is very large and the failures occur in the brace. For the specimens with  $r = 0.64$  this difference is much smaller (see [1]) and that makes that due to the well known thickness effect the crack starts not in the brace at the higher SNCF but in the chord with the lower SNCF.

In the  $\epsilon_r$ -N diagrams the results of these specimens are compared with the existing  $S_r$ -N curves for brace failure ( $t = 5$  mm) resp. chord failure ( $t = 12.5$  mm).

### 7.2.2 Mode of failure

The tests were ended when the crack length extended over a length equal to the side length of the brace parallel to the chord. Generally the cracks started at two corners, either in the brace or in the chord and grew together parallel to the chord axis.

In principle two types of failure occurred:

- in the brace
- in the chord

#### a. Brace failure

All the specimens with a brace thickness of 5 mm failed in the brace. The cracks initiated at the weld toe of the brace exactly at the corners. The cracks developed along the weld toe parallel to the chord and at the end of test perpendicular to the chord, the cracks at one side of the brace parallel to the chord grew together (see fig. 20).

#### b. Chord failure

All the specimens with a brace thickness of 8 mm failed in the chord. The crack always initiated at the weld toe at the corners. The cracks developed along the weld toe parallel the chord. At the end of test the cracks grew together at one side parallel to the chord and brace and chord were separate (see fig 21).

### 7.2.3 $\epsilon_r$ - N diagrams

In several codes the allowable  $S_r$ -N curve depends on the member thickness. Therefore separate  $\epsilon_r$ -N diagrams are given for each cracked member. The test results are given based on the  $\epsilon_r$   $h_s$  equivalent for comparison with the constant amplitude tests (see chapter 6.).

In the  $\epsilon_r$ -N diagram (see figs 16 and 17) four curves from literature are given.

- curve A: This curve represents the recommended characteristic  $S_r$ -N line for T-joints according to IIW document XV-582-85 (thickness dependent).  
The curve is valid for all types of joints independent of the stress ratio R. The characteristic (95% survival) fatigue strength is given in relation to the wall thickness t of the member under consideration [5]. In the figures the curve has been given in strain, using a correction factor of 1.1 due to the difference between SNCF and SCF ( $SCF \approx 1.1$  SNCF).
- curve C: This curve has been presented in the OTC paper 4999 as the mean value of the results of circular hollow section joints from the offshore research programme based on linear extrapolation [6]
- curve D: This curve represents the mean  $\epsilon$ -r-N curve for the experiments on rectangular hollow section joints (ECSC - Cidect programme [1,2]) based on quadratic extrapolation at the crack location.
- curve T: This design curve, presented in the OMAE paper '89 gives the revision of the preliminary fatigue design curves of DEN and an adopted "constant" thickness ratio for all thicknesses [7]. In the figures the curve has been given in strain, using a correction factor of 1.1 due to the difference between SNCF and SCF ( $SCF \approx 1.1$  SNCF).

Figures 18 and 19 show a comparison between the number of cycles for visually observed crack initiation  $N_i$  and failure  $N_f$  and the corresponding mean curves D and D'.

In these figures the curve D' represents the mean curve for crack initiation from the high cycle test results [1].

## 8. SUMMARY AND CONCLUSION

In this research programme 8 axially loaded T-joints between rectangular hollow sections have been tested under random loading.

The test series consists of specimens with chord dimensions of 200\*200\*12.5 and brace dimensions of 140\*140\*5 or 140\*140\*8. The geometrical parameters covered in this programme are  $\beta = 0.7$ ;  $2\gamma = 16$  and  $\tau = 0.4$  or  $0.64$ .

The specimens with a brace thickness of 5 mm were fillet welded and those with a brace thickness of 8 mm were butt welded. All specimens were made of steelgrade Fe 430 according to Euronorm 25-72.

Fatigue testing was carried out under random loading for two loading spectra  $P = F_{r \min} / F_{r \max} = 1/3$  or  $2/3$ .

The actual equivalent load range was determined by using the Miner rule and based on curve D which represents the mean results of the previous high cycle constant amplitude fatigue tests [1].

The aim of this experimental investigation is to compare the results of the fatigue behaviour of joints made of square hollow sections under random loading with the  $\epsilon_r$ -N and curves derived from previous high cycle and low cycle constant amplitude tests [1,2].

Furthermore the results are compared with various existing curves.

The conclusions from this random load fatigue investigation on T-joints can be summarized as follows:

- The maximum SNCF's are found in the brace at line A and in the chord at line C (see fig. 9) which is in agreement with previous results [1,2].
- All specimens showed higher SNCF values for the brace than for the chord (see also [1]). Nevertheless the specimens with  $\tau = 0.64$  failed in the chord due to the fact that the chord is thicker than the brace (thickness effect).

For the specimens with  $\tau = 0.4$  the difference between brace-SNCF and



the chord-SNCF is much larger than for the specimens with  $r = 0.64$ . Therefore, in spite of the thickness effect these specimens failed in the brace due to the higher SNCF

- Crack initiation starts at about 10% to 25% of the total fatigue life (see figs. 18 and 19).
- The fatigue tests under random loadings show that the  $\epsilon_r$ -N curve derived from the random test results ( see fig. 16 and 17) is less steep than the  $\epsilon_r$ -N curves for constant amplitude experiments (curve D). This may be due to a reduced damage of the smaller cycles in the random loading which are below the equivalent stress levels. However the number of test results is too small to draw firm conclusions.
- The IIW characteristic design curve A may be somewhat conservative for the small thicknesses  $t = 5$  mm with brace failures (fig. 16). However for larger thicknesses (fig. 17) the curve gives a lower bound of the results.
- No significant influence of the P-ratio has been found. However the number of test results is small.

#### Main conclusions

Using the equivalent stress approach all the test results of this random load fatigue programme are above the mean line of equivalent tests under constant amplitude loading tests (curve D).

Using the D-line for random loading seems to be on the safe side, at least for  $N > 10^5$  cycles.

## 9. References

- [1] Verheul A. :Fatigue behaviour of joints between rectangular  
Noordhoek C. hollow sections. T-joints part 1.  
Wardenier J. 1987, Stevin report 6-87-10/TNO-IBBC report  
Dutta D. Bi-87-118/63.5.3.820
- [2] Verheul A. :The low cycle fatigue behaviour of axially  
Wardenier J. loaded T-joints between rectangular hollow  
section.  
1989, Stevin report 25.68.89.22/A1, TNO-IBBC  
report BI-89-60/63.5.3820
- [3] Wingerde van A.M. :Fatigue behaviour of joints between rectangular  
Puthli R.S. hollow sections. T-joints part 2.  
Koning C.H.M. 1987, Stevin report 6-87-11/TNO-IBBC report  
Wardenier J. Bi-87-82/63.5.3.820  
Dutta .D
- [4] Delft van D.R.V. :A two-dimensional analysis of the stresses at  
the vicinity of the weld toes of welded  
tubular joints.  
1981, report 6-81-8, Stevin laboratory,  
Delft University of technology.
- [5] IIW-XVE :Recommended fatigue design procedure for  
hollow section joints.  
Doc. SC-XV-582-85/XIII-1158-85
- [6] Delft, van D.R.V. :Evaluating of the European fatigue.  
Noordhoek, C. Test data on large-sized welded Tubular joints  
Back, de J. for offshore structures.  
OTC-paper-4999-1985

- [7] Sharp J.V. :The fatigue performance of tubular joints in  
Thorpe T.W air and seawater.  
MaTSU, Harwell Laboratory, Oxfordshire, U.K.  
(presented during the OMAE 1989, but not  
included in the proceedings)

TEST SPECIMEN NUMBER	NOMINAL DIMENSIONS		$\beta$	$2\gamma$	$\tau$	WELD <sup>*</sup>	P RATIO
	CHORD $b_0 * h_0 * t_0$	BRACE $b_1 * h_1 * t_1$					
T25	200*200*12.5	140*140*5	0.7	16	0.4	FILLET WELD	1/3
T26							2/3
T27							1/3
T28							2/3
T33	200*200*12.5	140*140*8	0.7	16	0.64	BUTT WELD	1/3
T34							2/3
T35							2/3
T36							1/3

\*  $t < 8$  mm : fillet welds

$t > 8$  mm : butt welds

Table 1 : Review of the T-joint specimens

\*\*\*\*\*  
\*  
\* FATIGUE BEHAVIOUR OF JOINTS BETWEEN RECTANGULAR HOLLOW SECTIONS \*  
\* RANDOM LOADING \*  
\*\*\*\*\*

$\epsilon_{r_{hs}}$  AND SNCF BASED ON CRACK LOCATION ( QUADRATICALLY EXTRAPOLATED )




TEST	CHORD	BRACE	P	$F_{r_{nom}}$	$F_{r_{nom}}$	$F_{r_{nom}}$	$S_{r_{ab}}$	$S_{r_{ab}}$	$S_{r_{ab}}$	$\epsilon_{r_{ab}}$	$\epsilon_{r_{ab}}$	$\epsilon_{r_{ab}}$	$\epsilon_{r_{hs}}$		$\epsilon_{r_{hs}}$		$\epsilon_{r_{hs}}$		SNCF		Ni $\ast 10^6$	Nf $\ast 10^6$	MODE OF FAILURE
				max.	min.	equi.	max.	min.	equi.	max.	min.	equi.	maximum		minimum		equivalent		chord	brace			
				KN	KN	KN	N/mm	N/mm	N/mm				chord	brace	chord	brace	chord	brace					
T25	200*200 t=12.5	140*140 t=5	1/3	280	108	122	106.3	41.0	46.4	506	195	221	1097	4236	424	1635	479	1849	2.17	8.37	0.046	0.891	BRACE
T26			2/3	135	98	100	51.5	37.1	38.0	245	177	181	600	1967	433	1419	443	1453	2.45	8.03	0.151	6.141	BRACE
T27			1/3	154	57	69	60.8	22.7	27.3	289	108	130	634	2876	237	1072	285	1292	2.19	9.94	1.704	9.715	BRACE <sup>1</sup>
T28			2/3	198	133	141	75.0	50.4	53.6	357	204	255	735	2635	494	1772	525	1881	2.06	7.38	0.024	0.314	BRACE
T33		t=8	1/3	276	101	121	67.5	24.8	29.6	321	118	141	1668	--	612	--	732	--	5.19	-	0.475	3.279	CHORD
T34			2/3	226	158	166	56.9	40.0	41.8	271	190	199	1392	—	975	—	1022	—	5.14	-	0.088	0.468	CHORD
T35			2/3	143	98	103	37.5	25.9	27.1	179	123	129	1019	—	703	—	736	—	5.71	-	0.235	2.694	CHORD
T36			1/3	376	141	161	93.2	35.0	39.9	444	166	190	2655	—	996	—	1137	—	5.98	-	0.021	1.341	CHORD

Ni= crack initiation

Nf= end of test (crack through)

<sup>1</sup> run out

Table 2 : Test results with quadratically extrapolated HSSNR and SNCF , based on crack location

test spec.	chord ) <sup>1</sup> (b <sub>0</sub> *h <sub>0</sub> *t <sub>0</sub> )	brace ) <sup>1</sup> (b <sub>1</sub> *h <sub>1</sub> *t <sub>1</sub> )					A <sub>0</sub> (mm)	A <sub>1</sub> (mm)			f <sub>y0</sub> • N/mm2	f <sub>y1</sub> • N/mm2	f <sub>u0</sub> x N/mm2	f <sub>u1</sub> x N/mm2	ε <sub>0</sub> ** %	ε <sub>1</sub> ** %
			t <sub>0 4</sub>	t <sub>1 3</sub>	r <sub>0 0</sub>	r <sub>1 0</sub>			a <sub>v</sub>	a <sub>h</sub>						
T25	200.6*200.6*12.7	140*140*4.97	14.9	6.0	15.24	5.98	9240	2595	6.56	9.16	314	310	462	437	33	42
T26	200.6*200.6*12.7	140*140*4.97	„	„	„	„	„	„	6.99	8.25	„	„	„	„	„	„
T27	200.6*200.6*12.7	140*140*4.97	„	„	„	„	„	„	6.73	8.99	„	„	„	„	„	„
T28	200.7*200.7*12.8	140*140*4.97	„	„	15.44	„	9059	„	6.78	9.66	333	„	467	„	35	„
T33	200.6*200.6*12.6	140*140*7.6	14.8	8.9	15.04	10.11	9320	3939	8.28	4.91	324	296	466	431	33	39
T34	200.6*200.6*12.6	140*140*7.6	„	„	„	„	„	„	8.33	3.67	„	„	„	„	„	„
T35	200.6*200.6*12.6	140*140*7.6	„	„	„	„	„	„	10.24	4.13	„	„	„	„	„	„
T36	200.6*200.6*12.7	140*140*7.6	„	„	15.24	„	9240	„	8.46	5.36	314	„	462	„	„	31

+ average values in the corners

• stub column tests

x tensile test (dp5)

\*\* elongation

)<sup>1</sup> The dimensions have been based on the average measured dimensions for each delivered RHS length.

Table 3 : Measured dimensions (mm) and mechanical properties

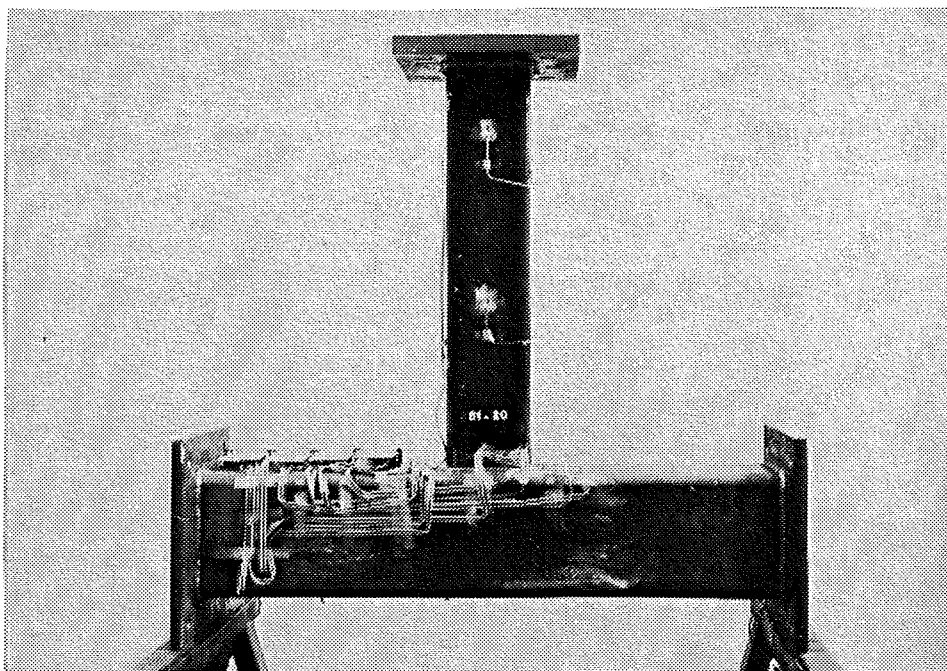


Fig. 1 : T-joint specimen (t= 8 mm)

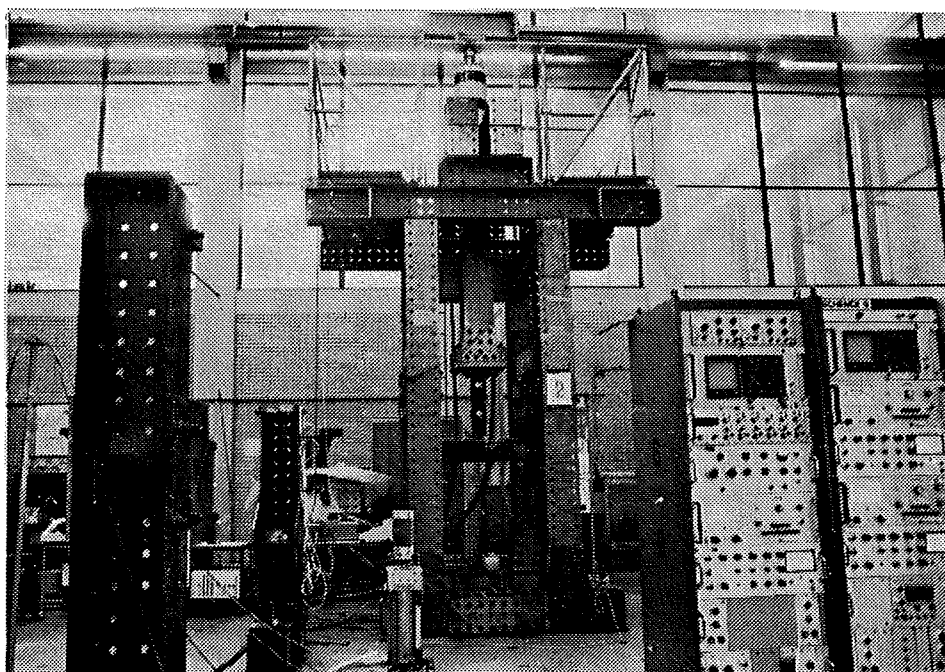
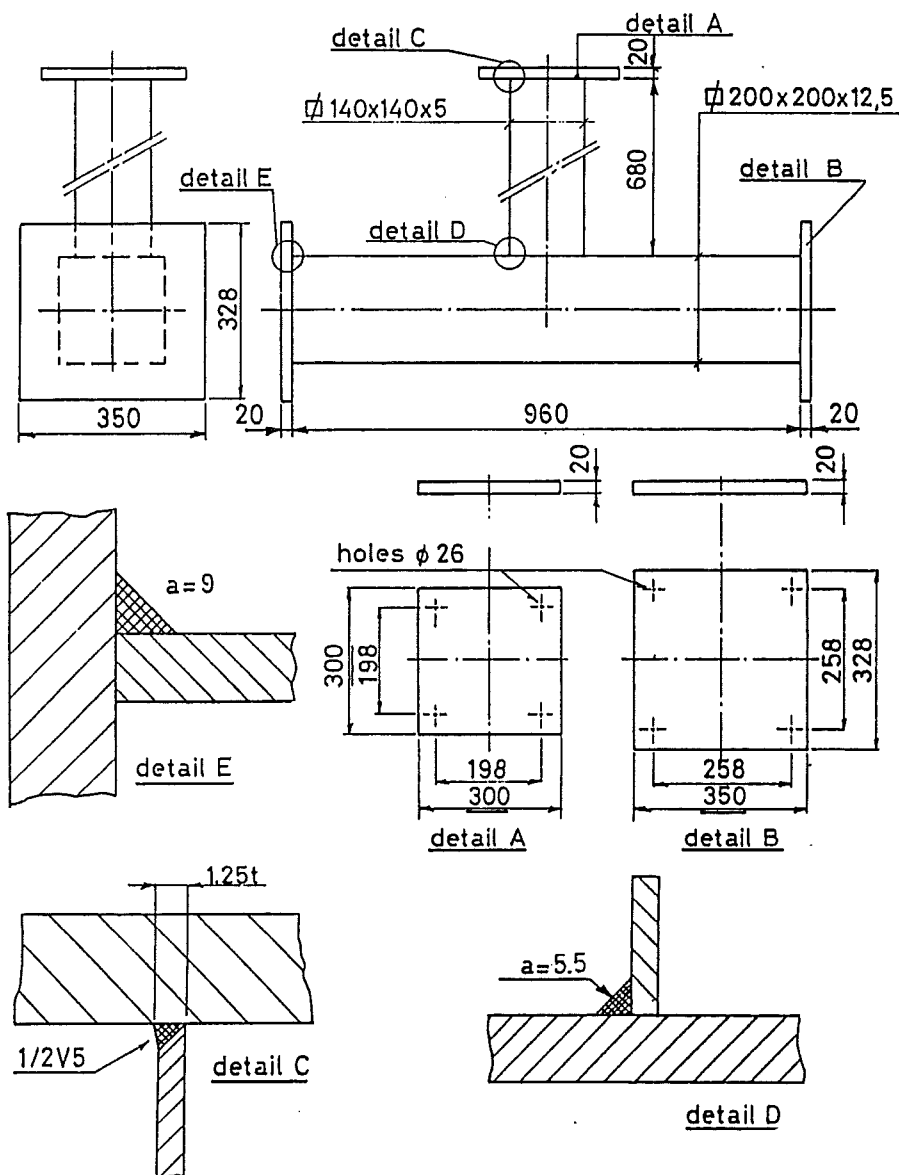


Fig. 2 : Test rig for T-joint specimens

# FATIGUE BEHAVIOUR OF JOINTS BETWEEN RECTANGULAR HOLLOW SECTIONS




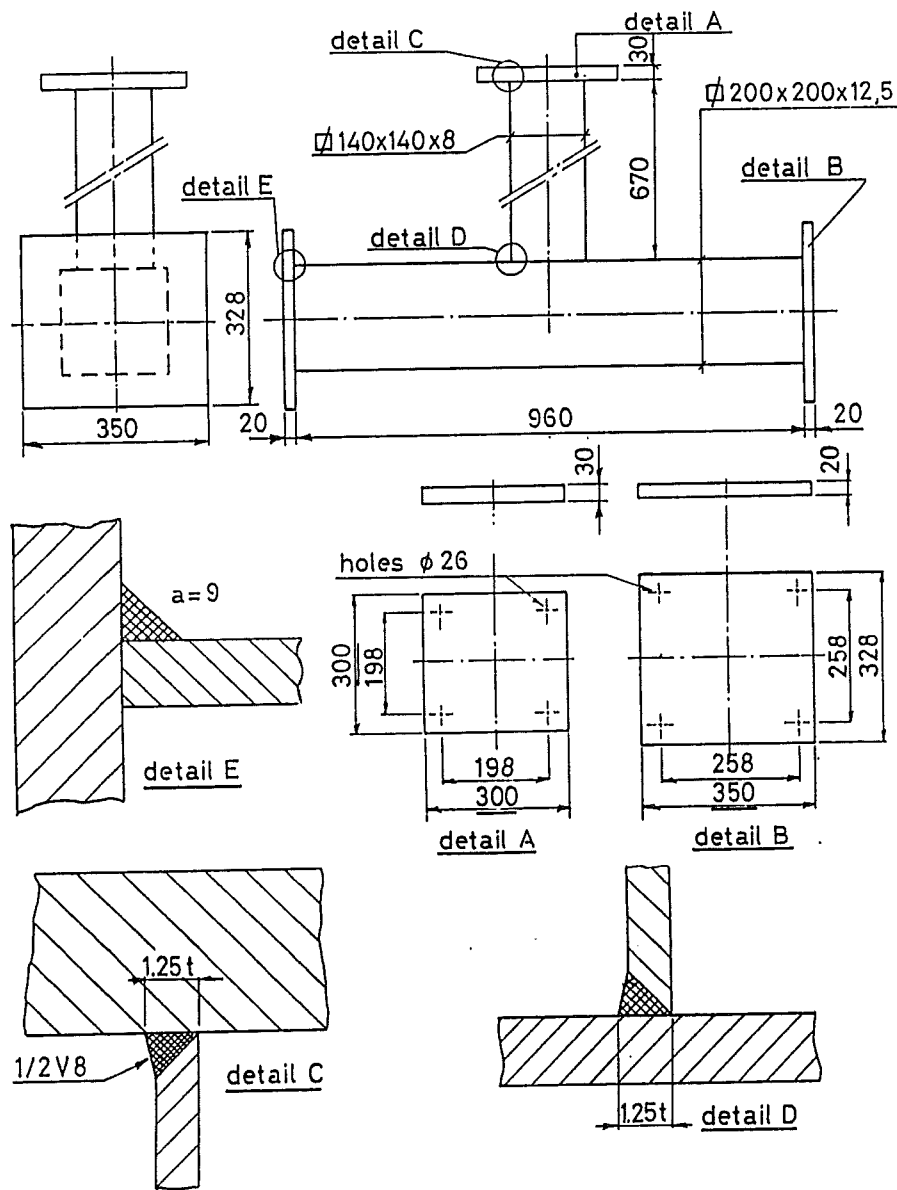
number	20	STEVINLABORATORIUM 
steel grade	Fe 430-C or D	
	endplate : Fe 360	
tolerances	max. angular divergence = 1/4°	
	max. distance center lines = 1 mm	

Fig. 3 : Configuration of the T-joint specimens. (wall thickness brace 5 mm)



# FATIGUE BEHAVIOUR OF JOINTS BETWEEN RECTANGULAR HOLLOW SECTIONS



number	20	STE VINLABORATORIUM <b>TU Delft</b>
steel grade	Fe 430-C or D	
	endplate: Fe 360	
tolerances	max. angular divergence = $1/4^\circ$ max. distance center lines = 1mm	

Fig. 4 : Configuration of the T-joint specimens. (wall thickness brace 8 mm)

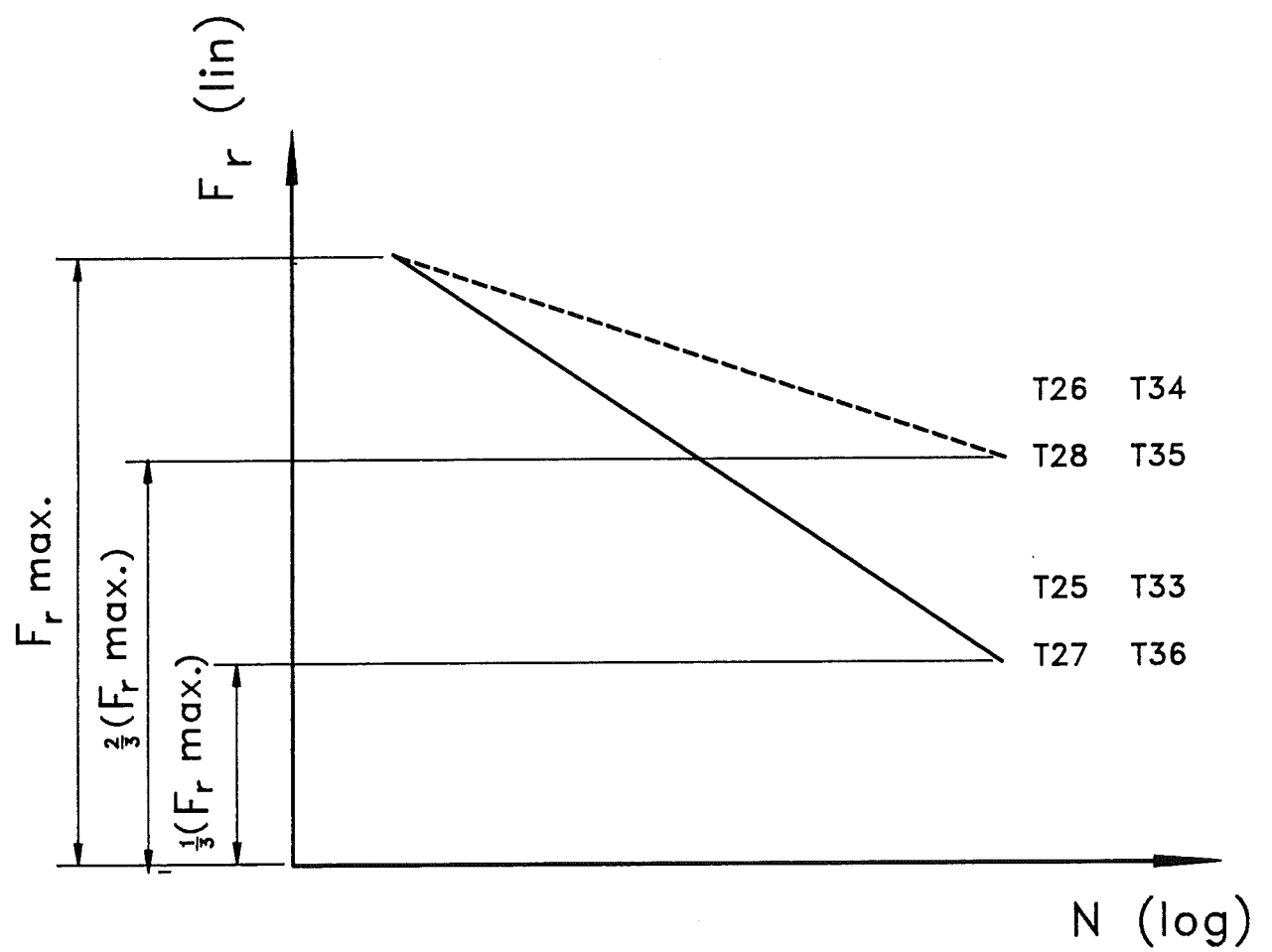


Fig. 5 : The applied load spectra and the specimens to be tested.

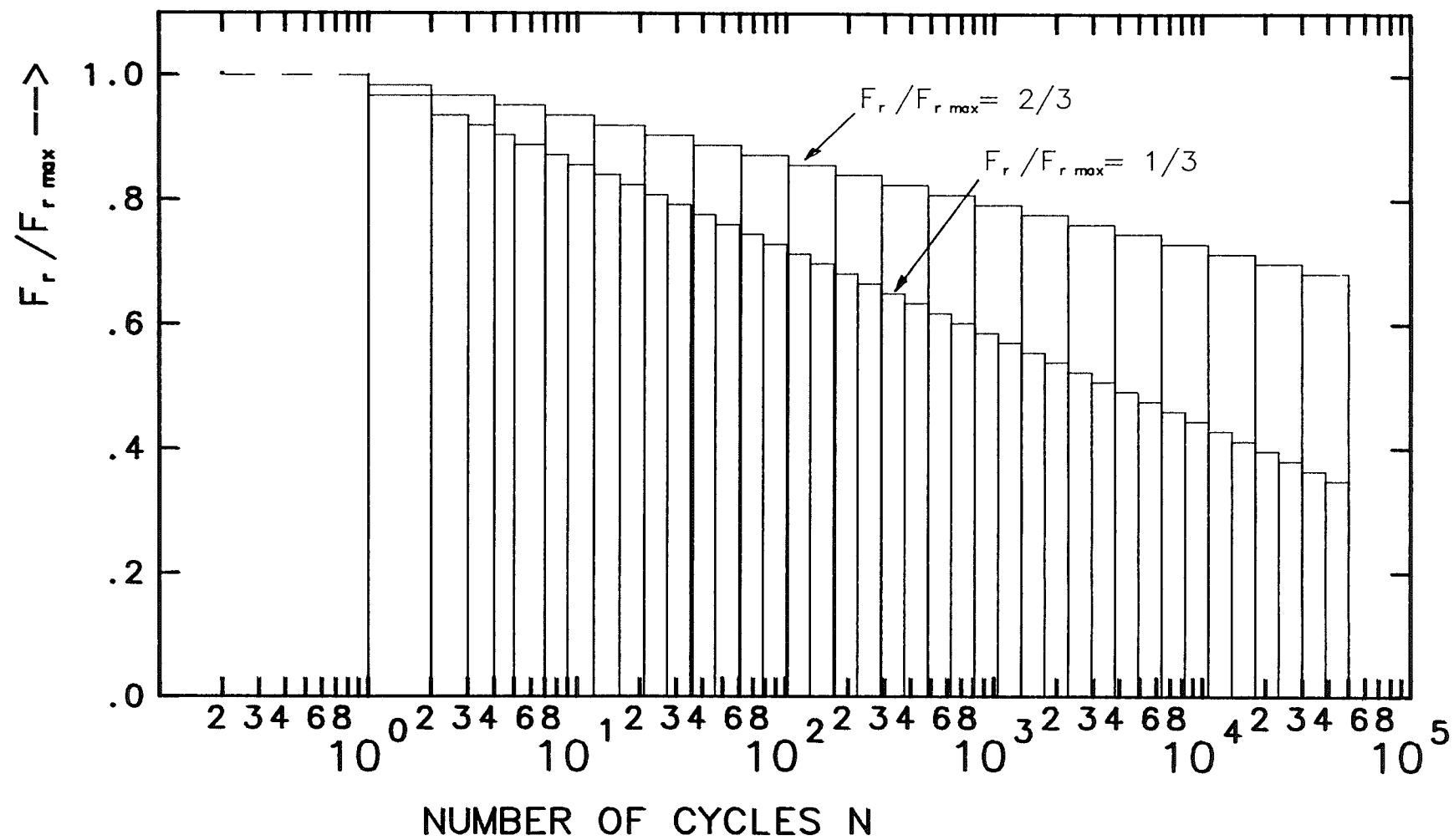


Fig. 6 : The load spectra divided in to blocks



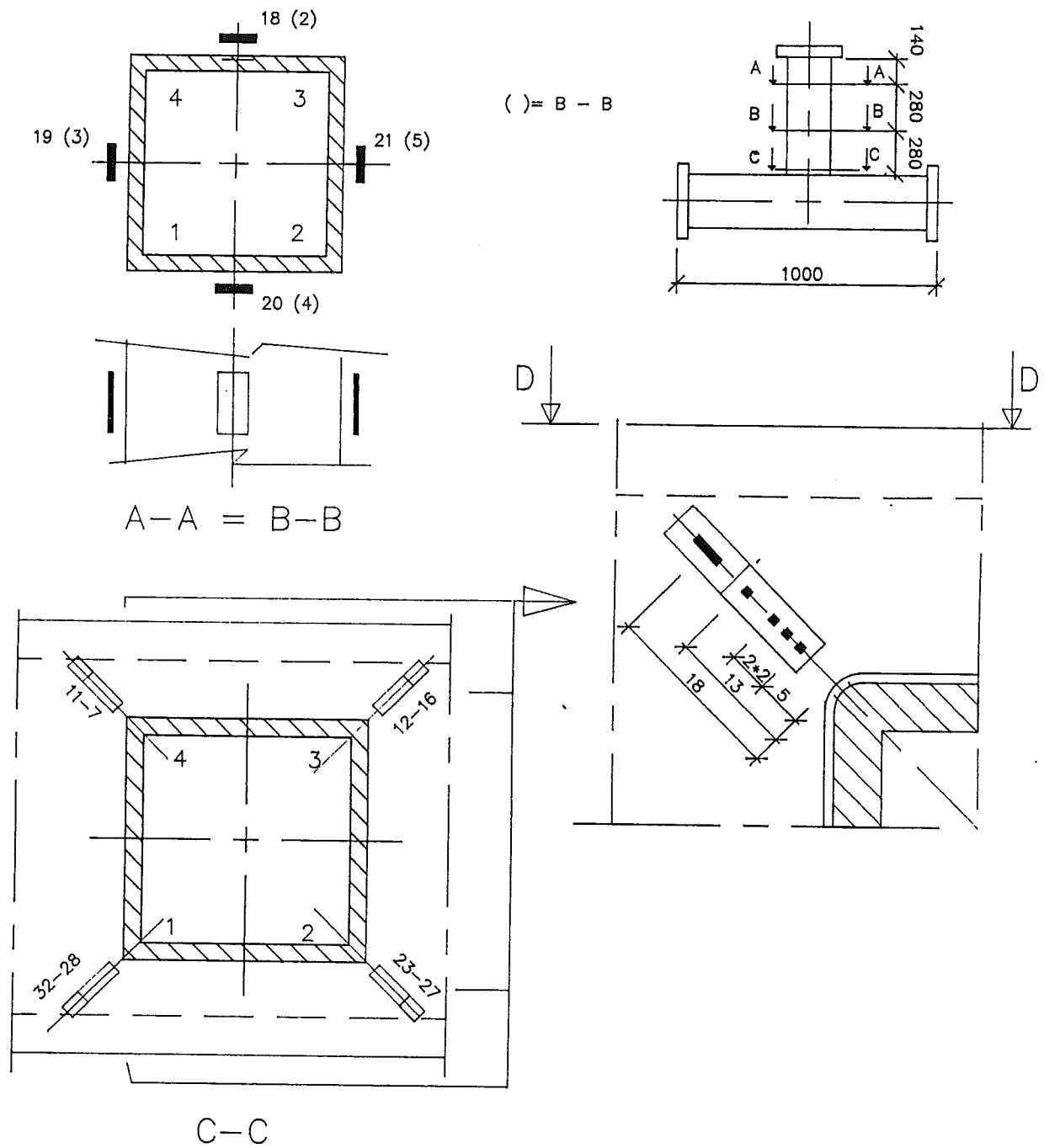


Fig. 8 : Location of the strain gauges of the specimens T 33 to T 36

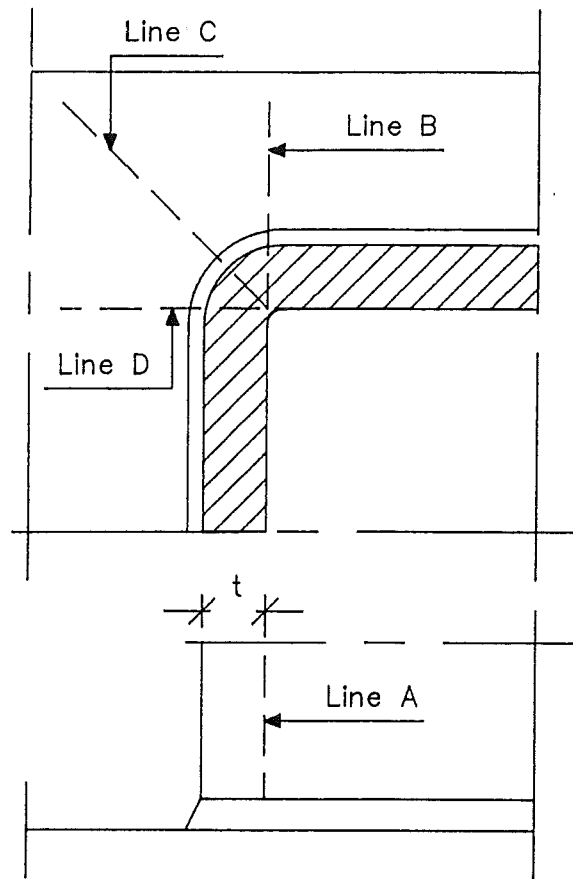


Fig. 9 : Location of the extrapolation lines

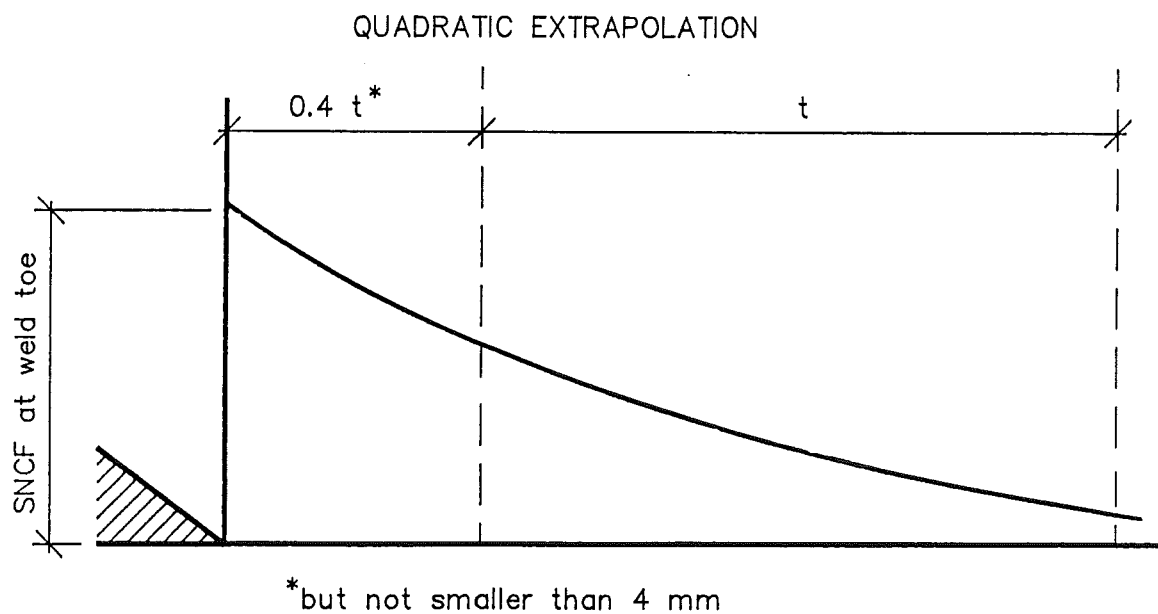


Fig.10 : Method of quadratic extrapolation

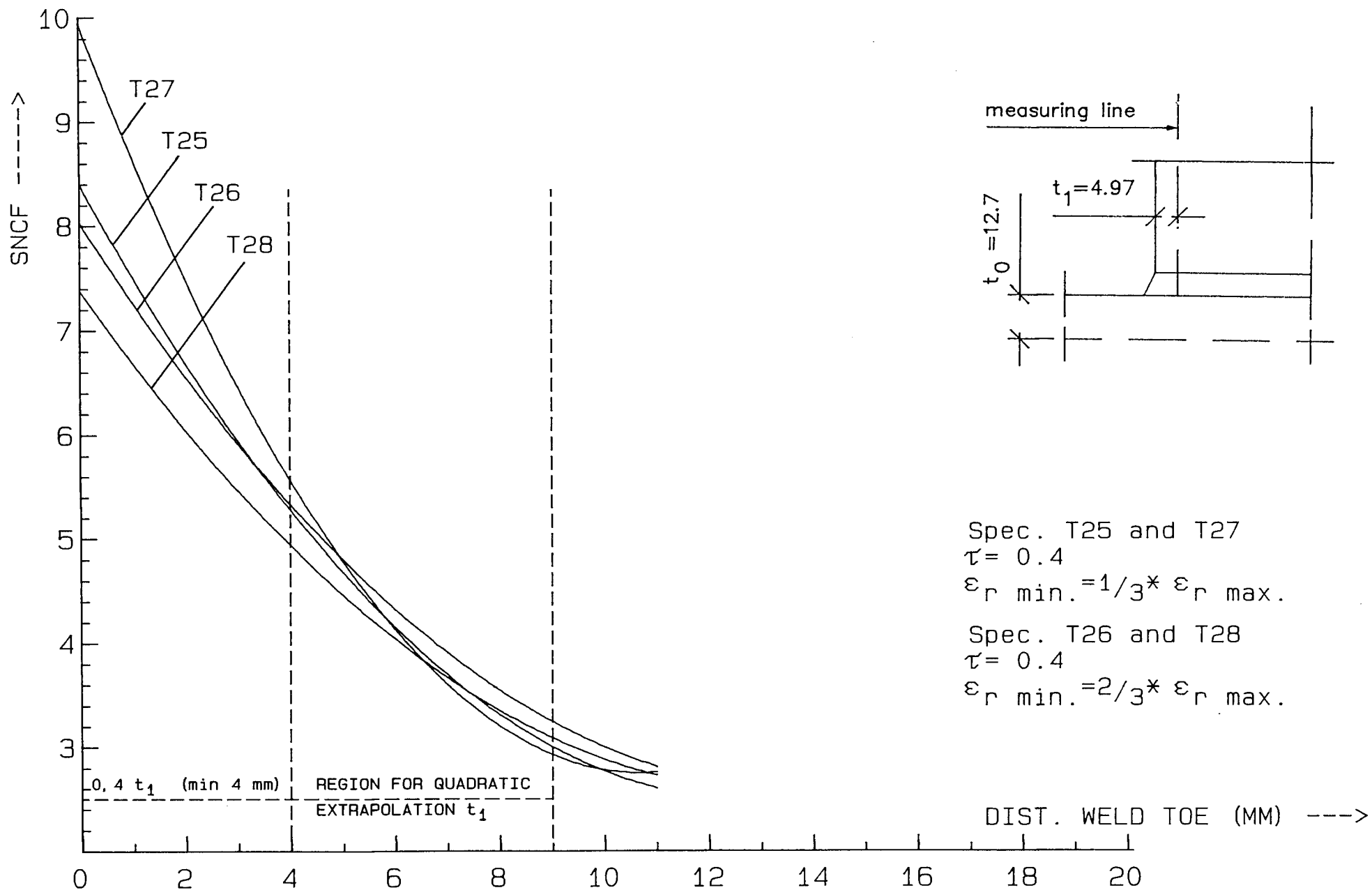


Fig.11 : SNCF DISTRIBUTION (BRACE) PARALLEL TO THE LONGITUDINAL AXIS OF THE BRACE  
 SPEC. T25 TO 28 - LINE A - SNCF BASED ON CRACK LOCATION

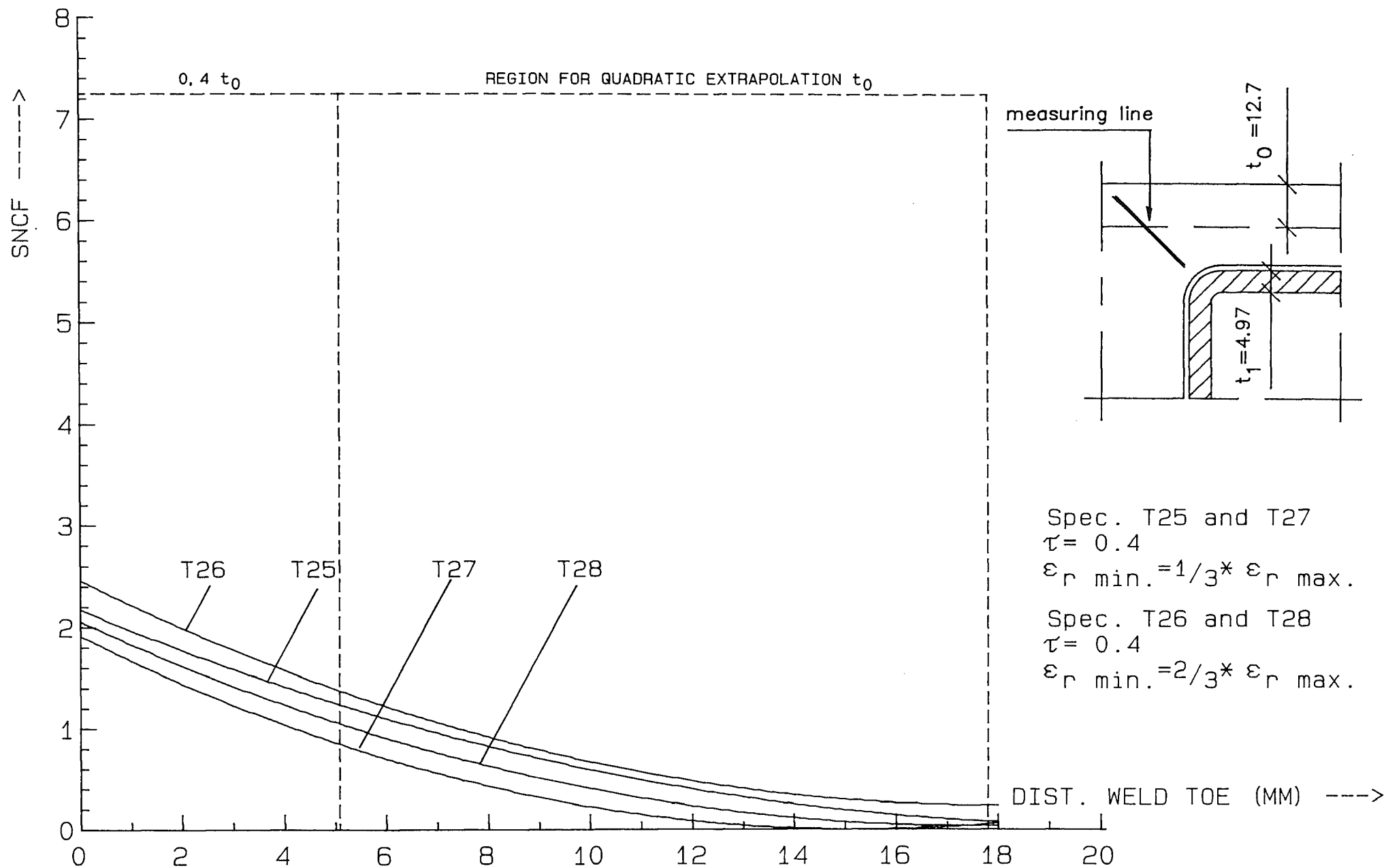


Fig. 12 : SNCF DISTRIBUTION (CHORD) 45 TO THE LONGITUDINAL AXIS OF THE CHORD  
 SPEC. T25 TO 28 - LINE C



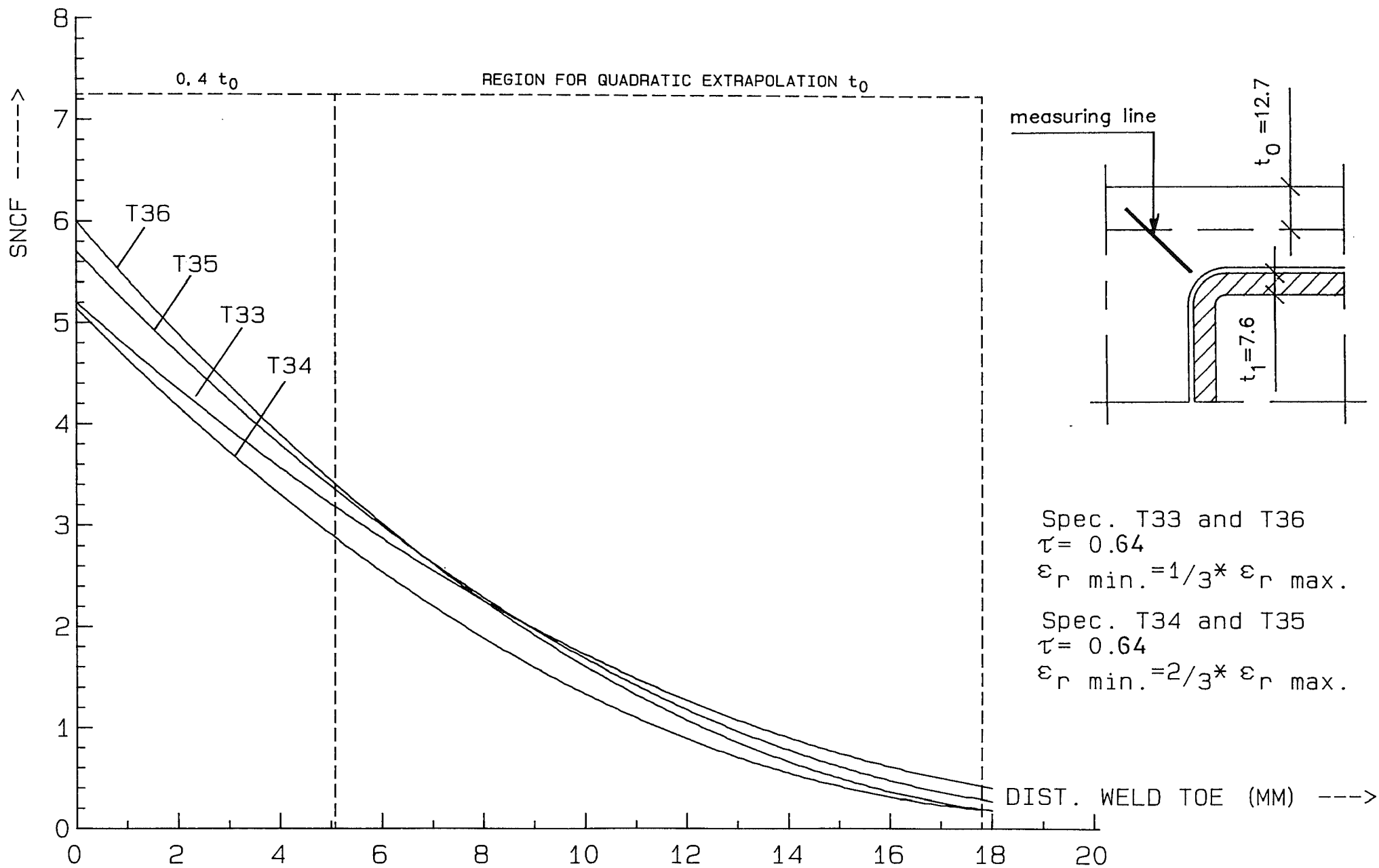


Fig. 13 : SNCF DISTRIBUTION (CHORD) 45 TO THE LONGITUDINAL AXIS OF THE CHORD  
 SPEC. T33 TO 36 - LINE C - SNCF BASED ON CRACK LOCATION

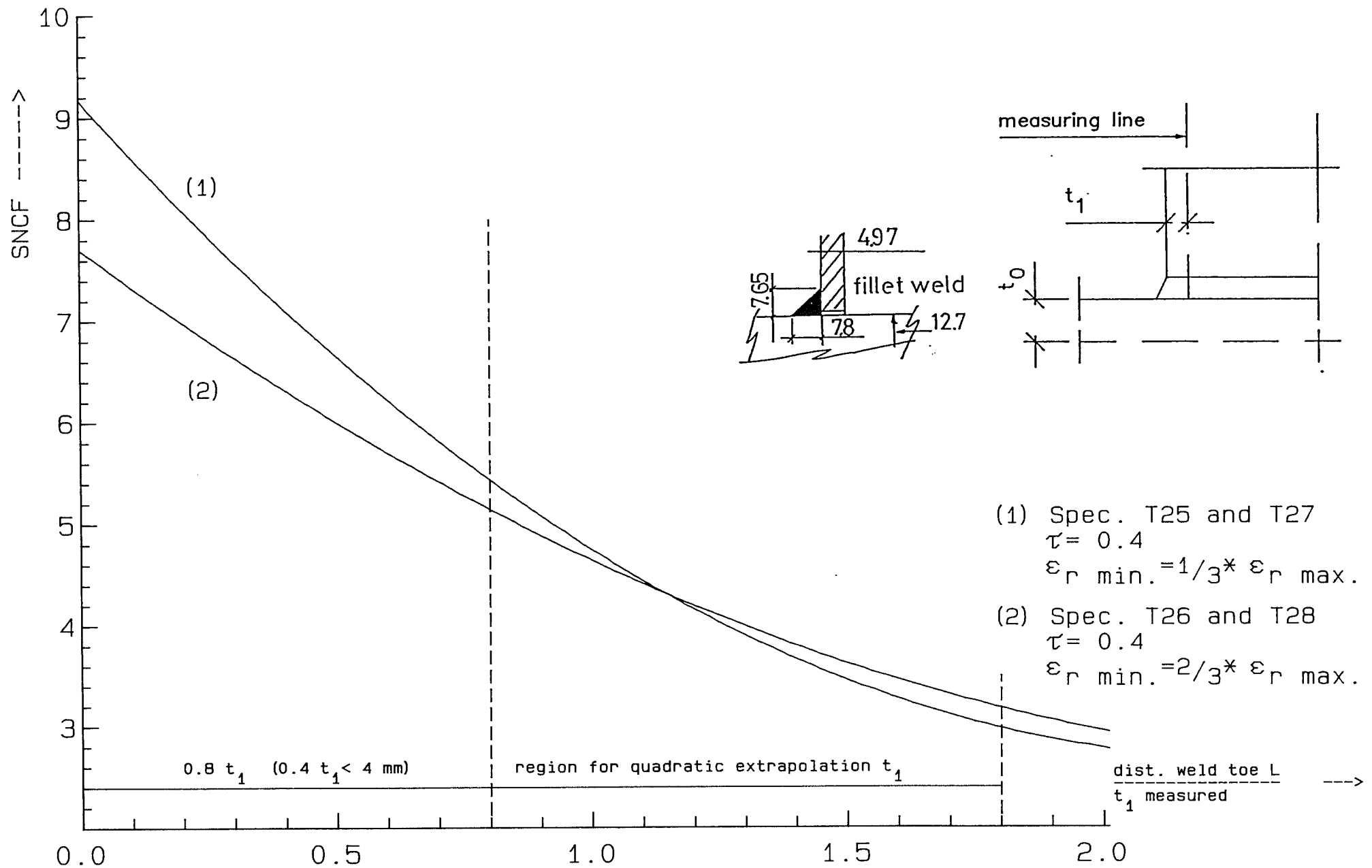


Fig.14: Comparison of the average SNCF distribution of each series under consideration - line A

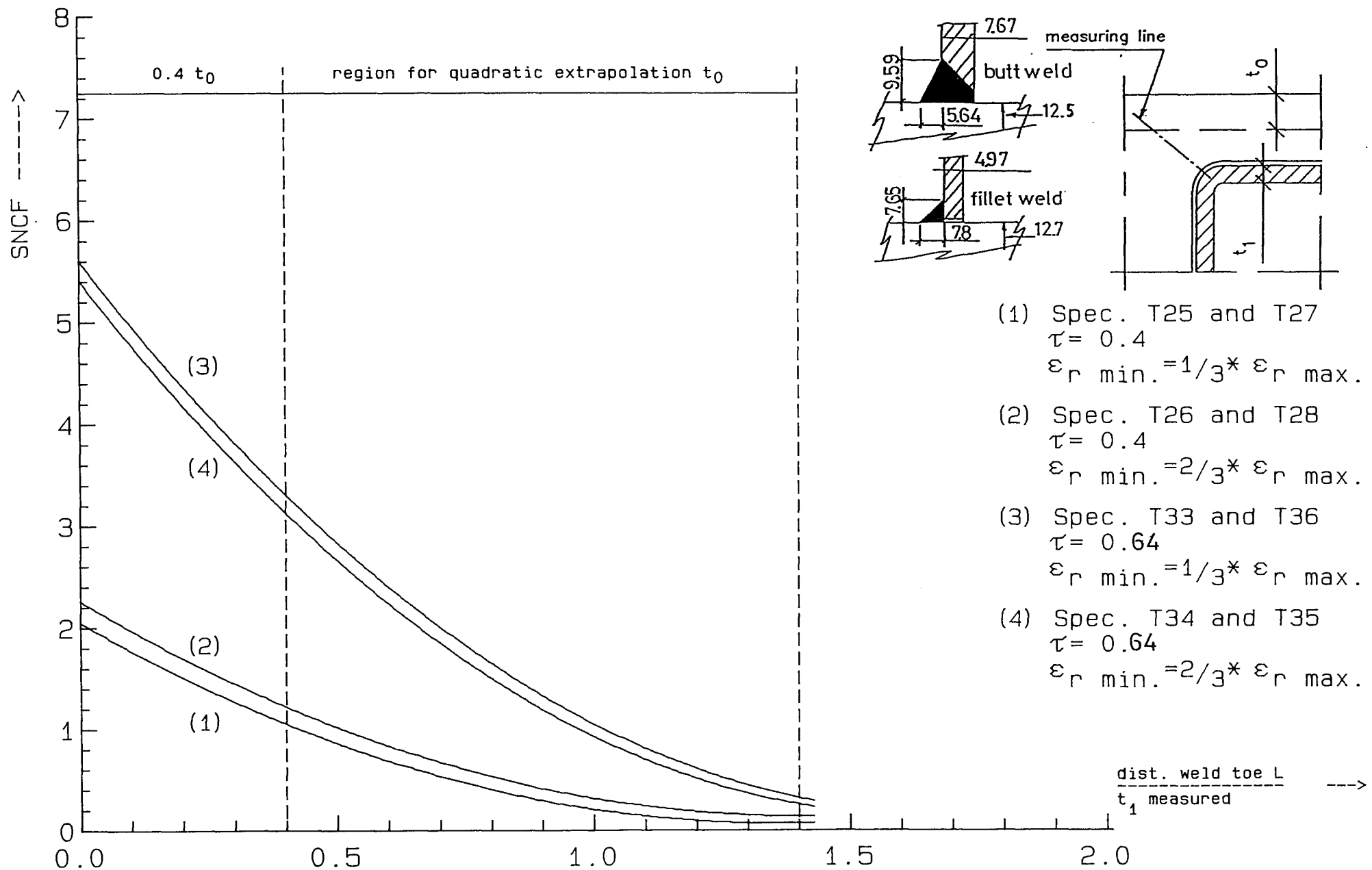
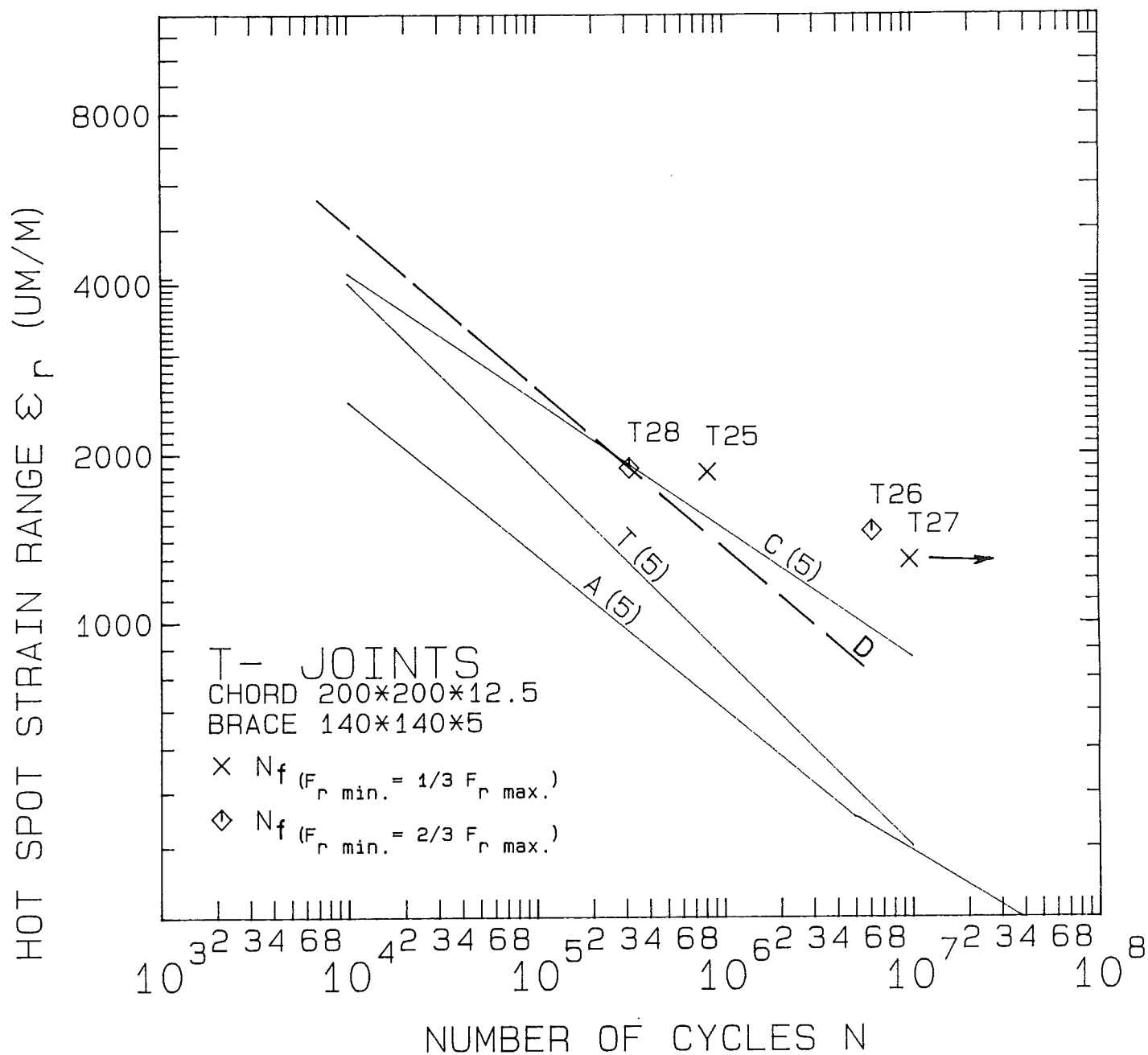


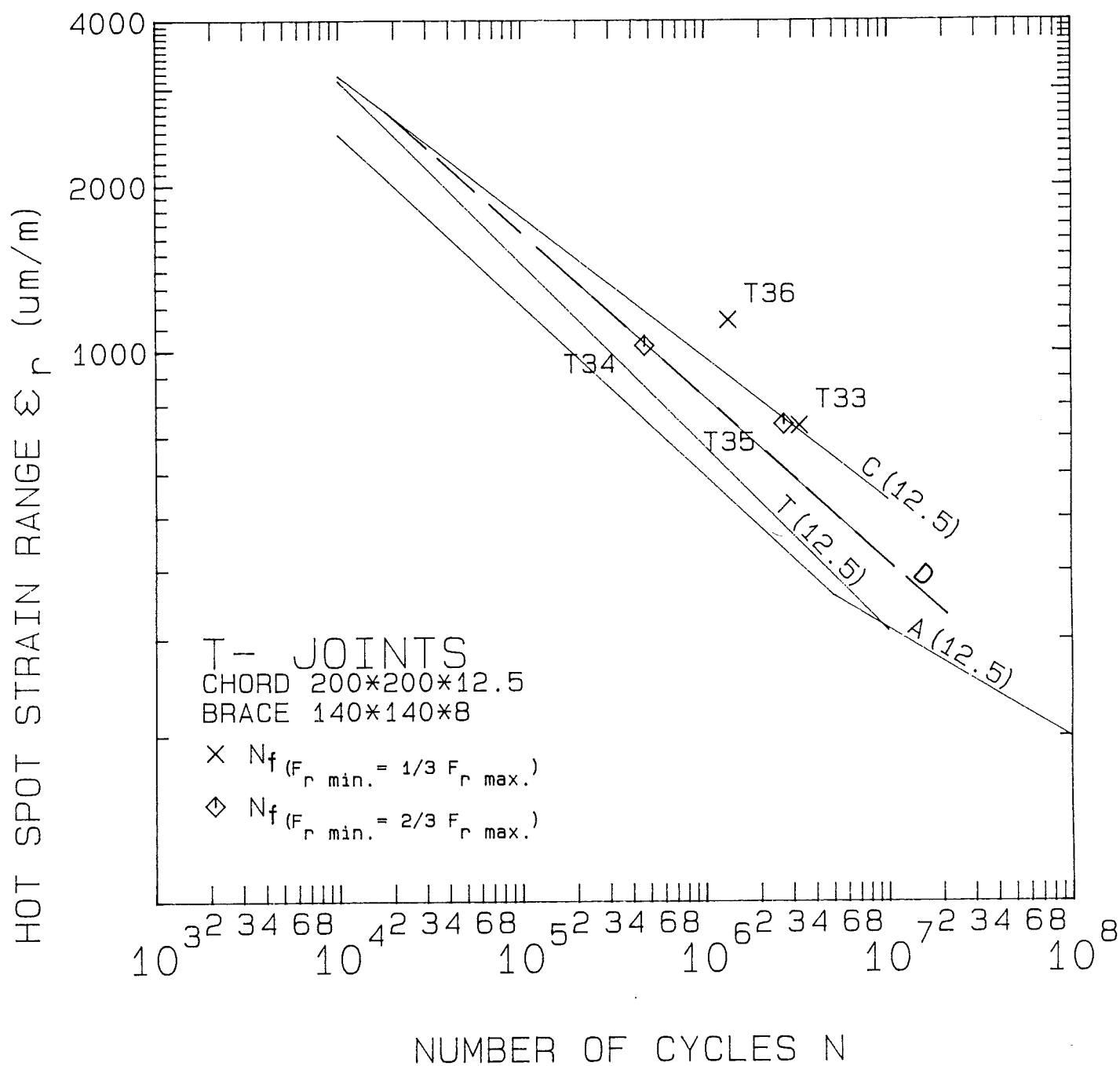
Fig.15: Comparison of the average SNCF distribution of each series under consideration - line c



FAILURE IN BRACE

QUADRATICALLY EXTRAPOLATED HSSNR BASED ON CRACK LOCATION

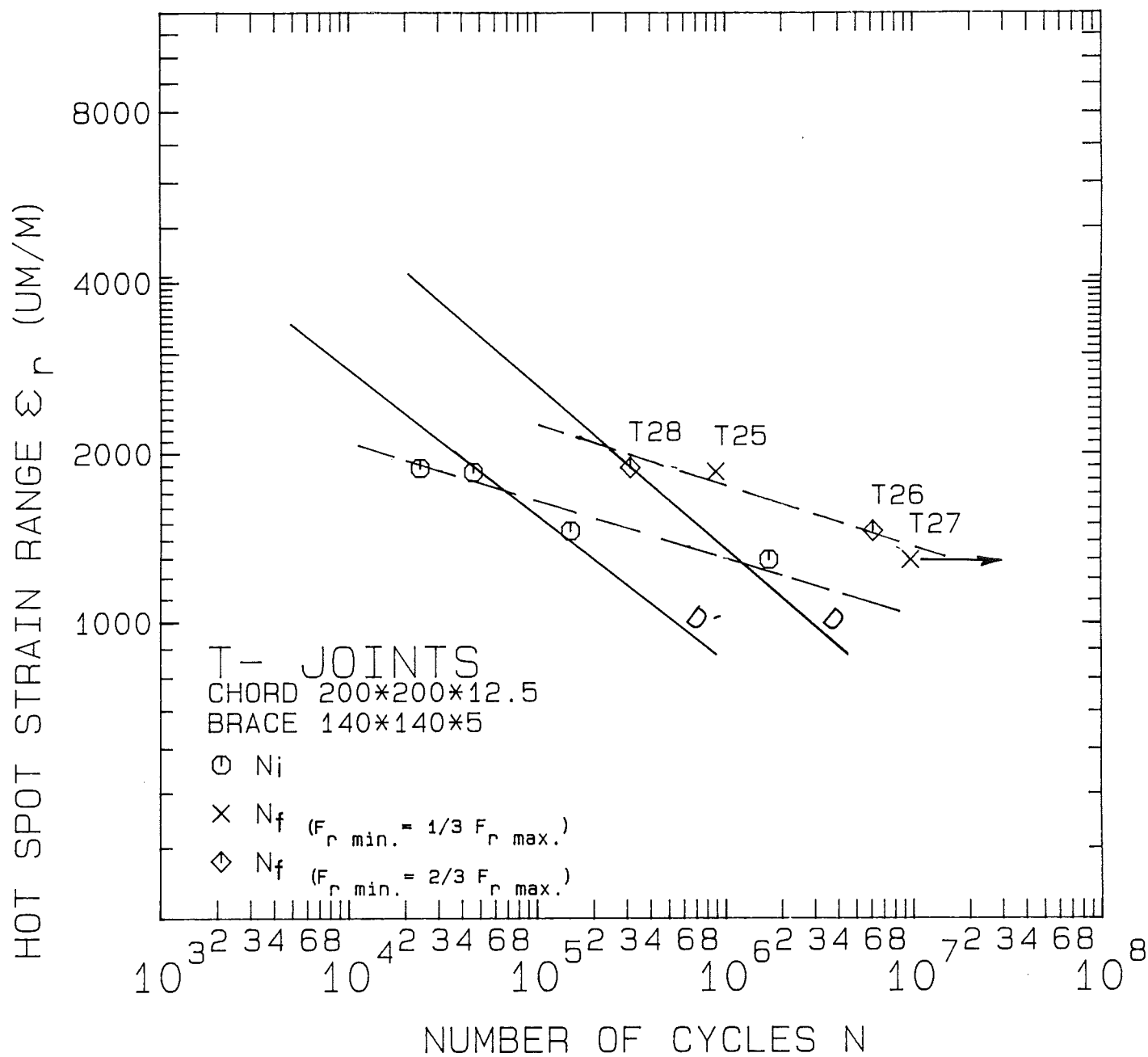
FIG. 16 : COMPARISON OF RANDOM LOAD FATIGUE RESULTS (HSSR) WITH EXISTING CURVES

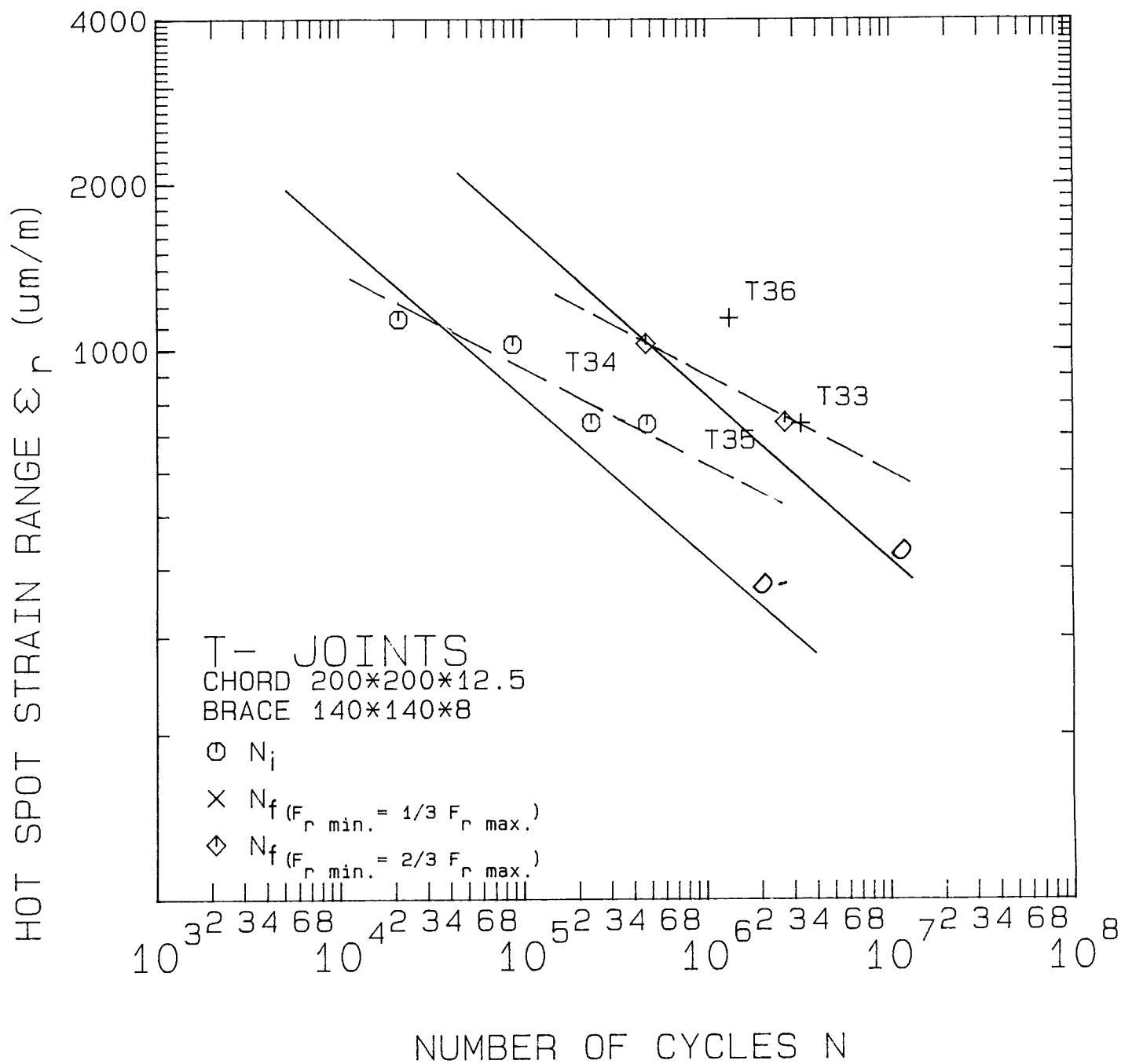


FAILURE IN CHORD

QUADRATICALLY EXTRAPOLATED HSSNR BASED ON CRACK LOCATION

FIG. 17 : COMPARISON OF RANDOM LOAD FATIGUE RESULTS  
 (HSSR) WITH EXISTING CURVES





FAILURE IN CHORD

QUADRATICALLY EXTRAPOLATED HSSNR BASED ON CRACK LOCATION

FIG. 19 : RELATION BETWEEN  $N_i$  AND  $N_f$

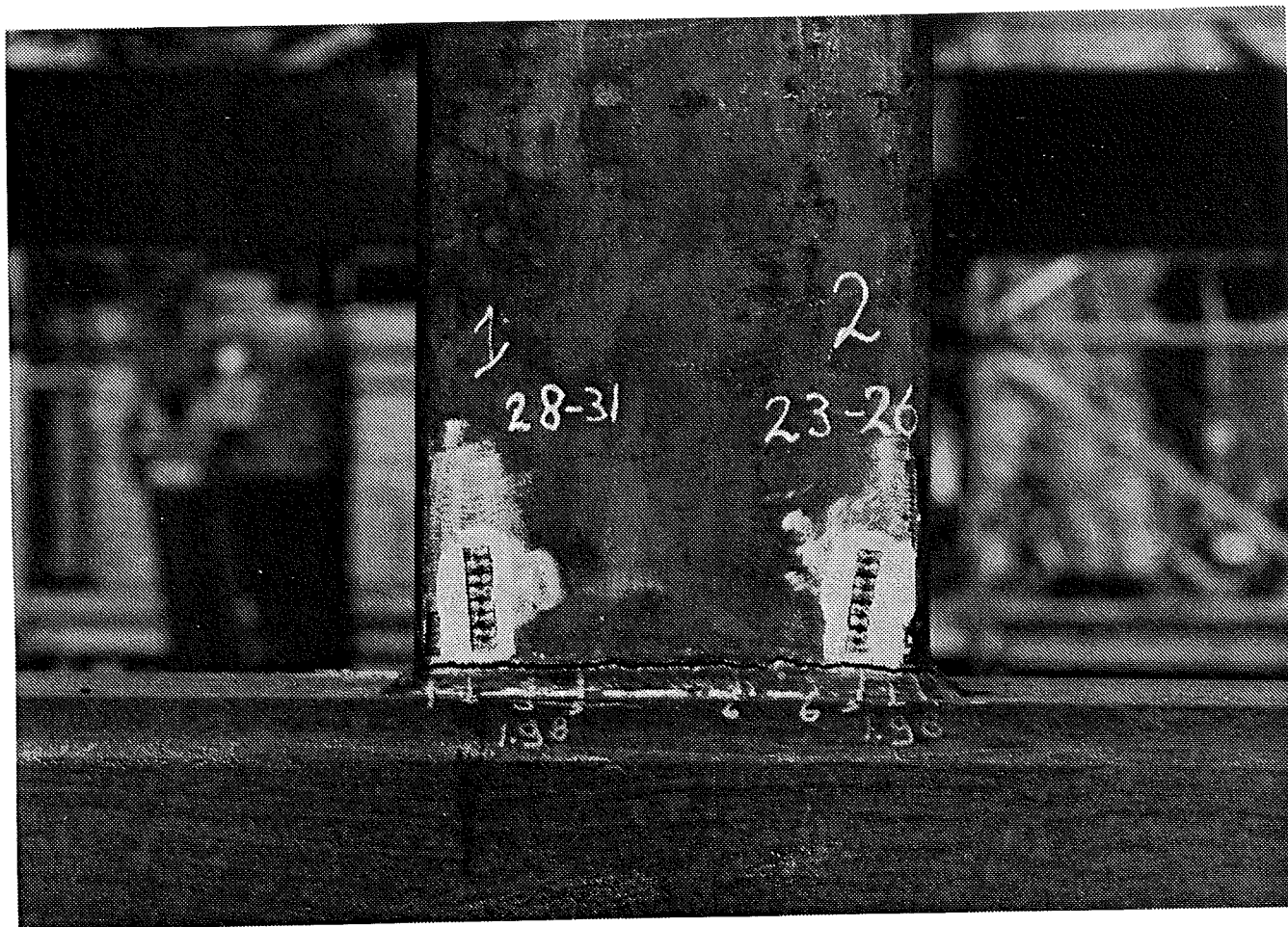


Fig.20: Typical crack shape of a T-joint specimen (brace thickness 5 mm)

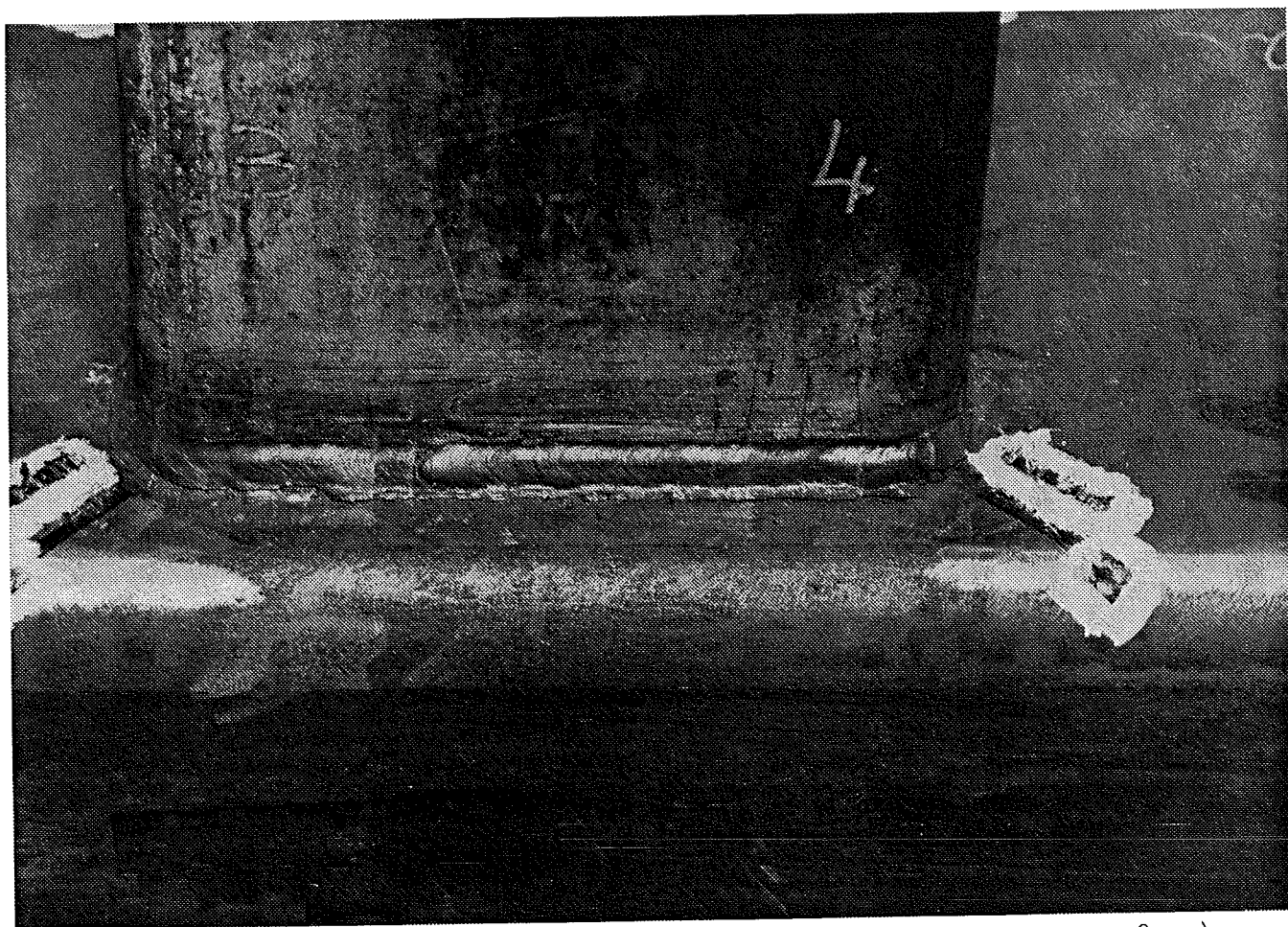


Fig.21 : Typical crack shape of a T-joint specimen (brace thickness 8 mm)



APPENDIX I

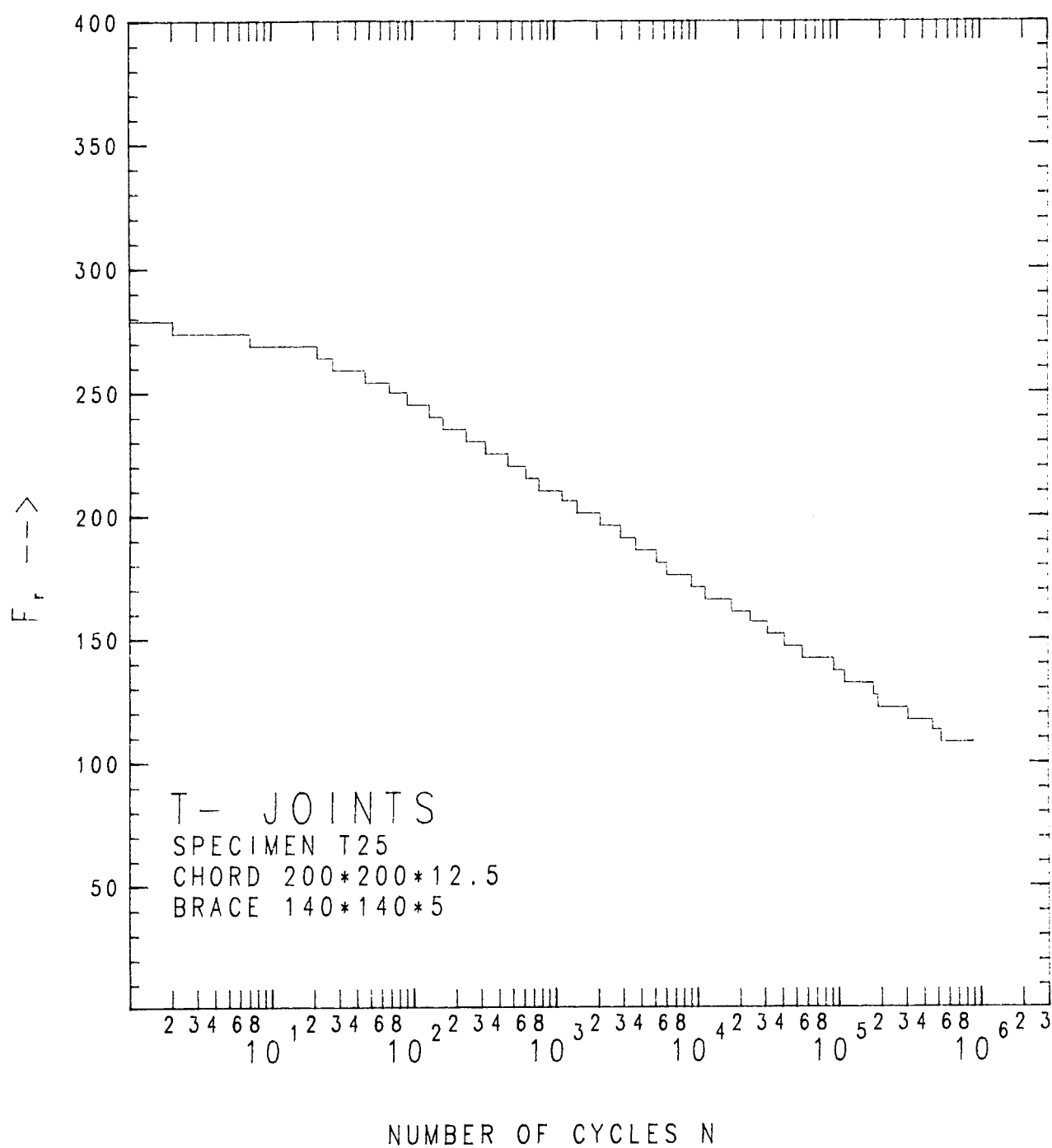


Fig. 22 : Load spectrum for T-joint T25

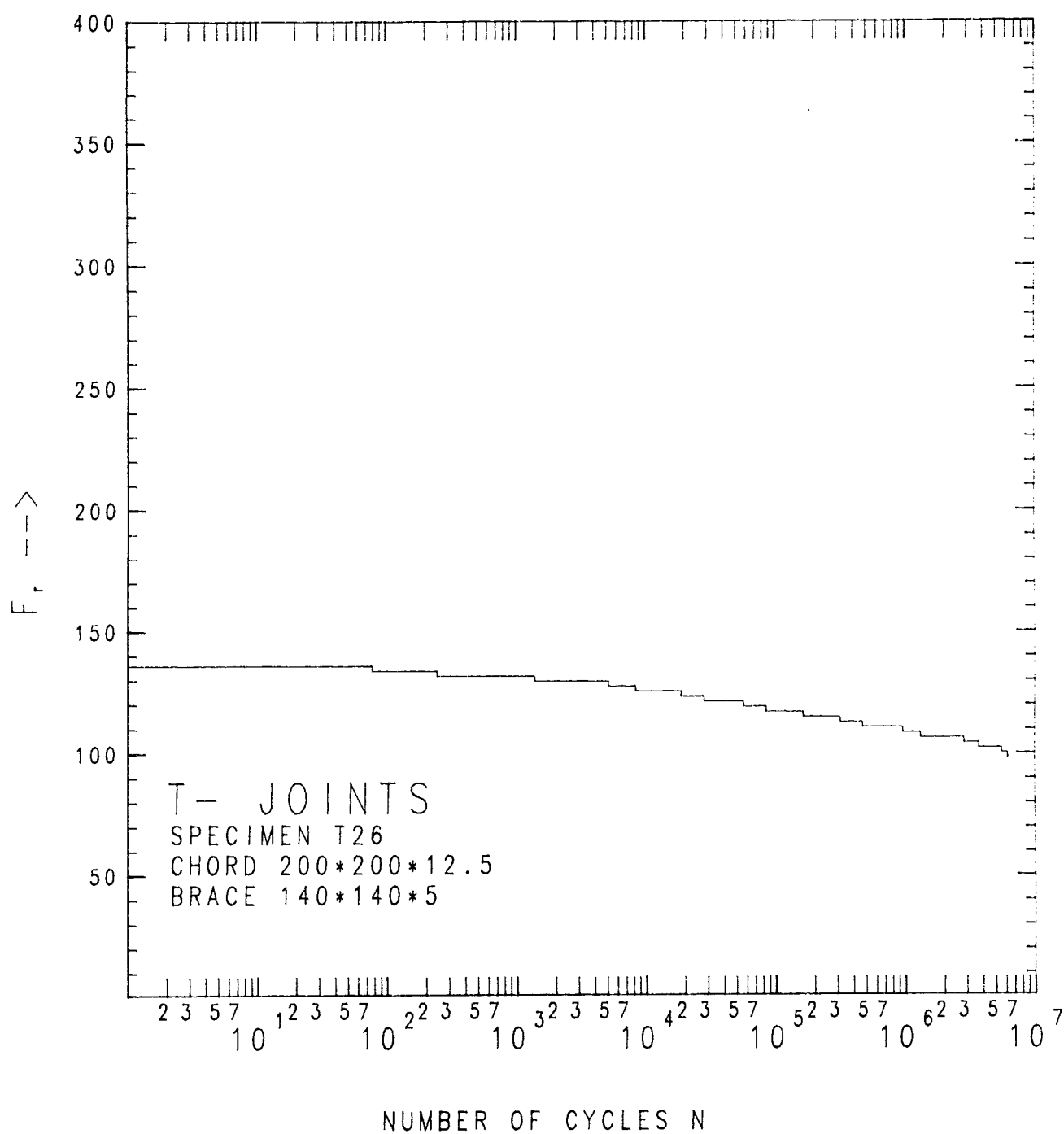


Fig. 23 : Load spectrum for T-joint T26

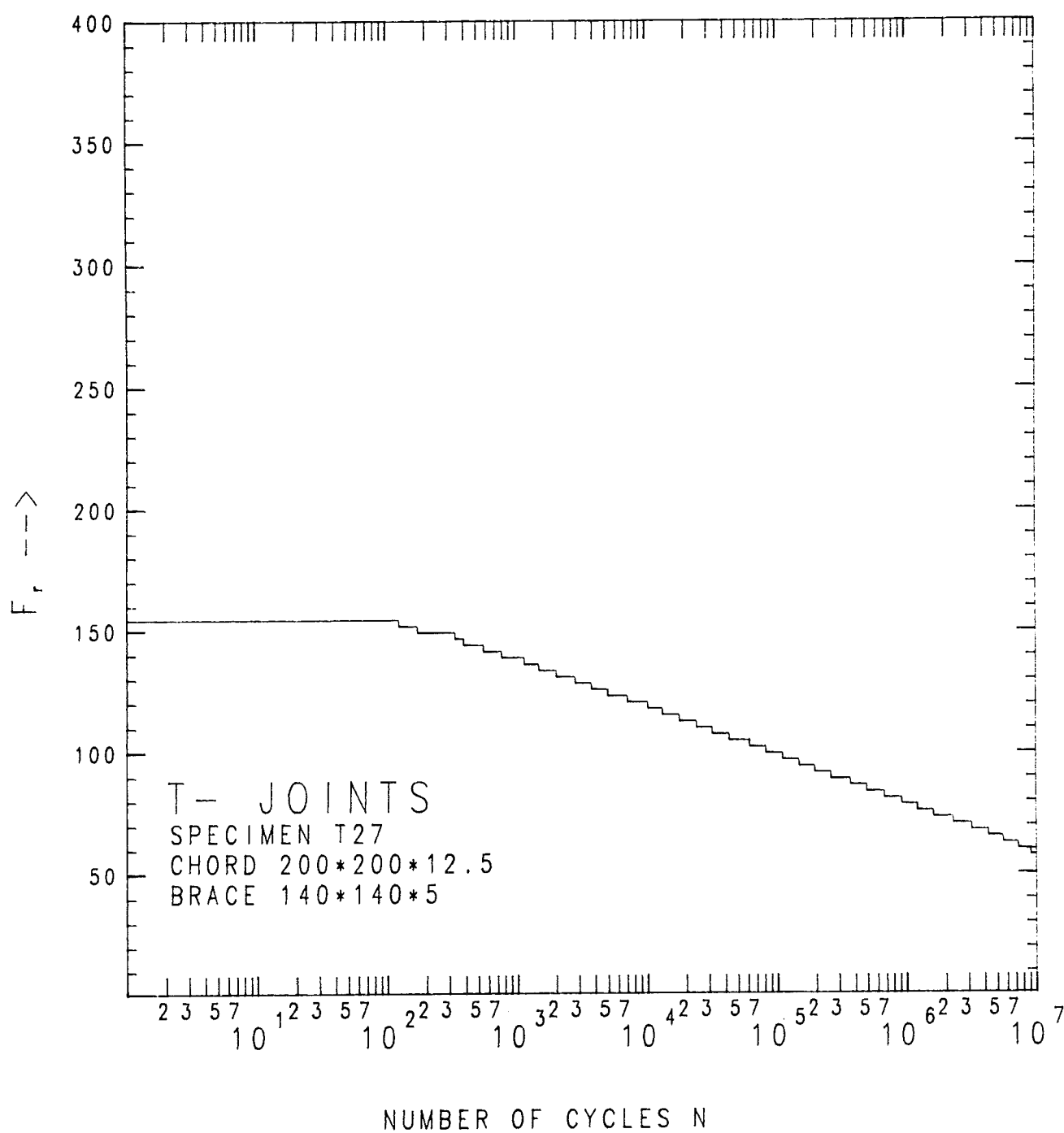


Fig. 24 : Load spectrum for T-joint T27

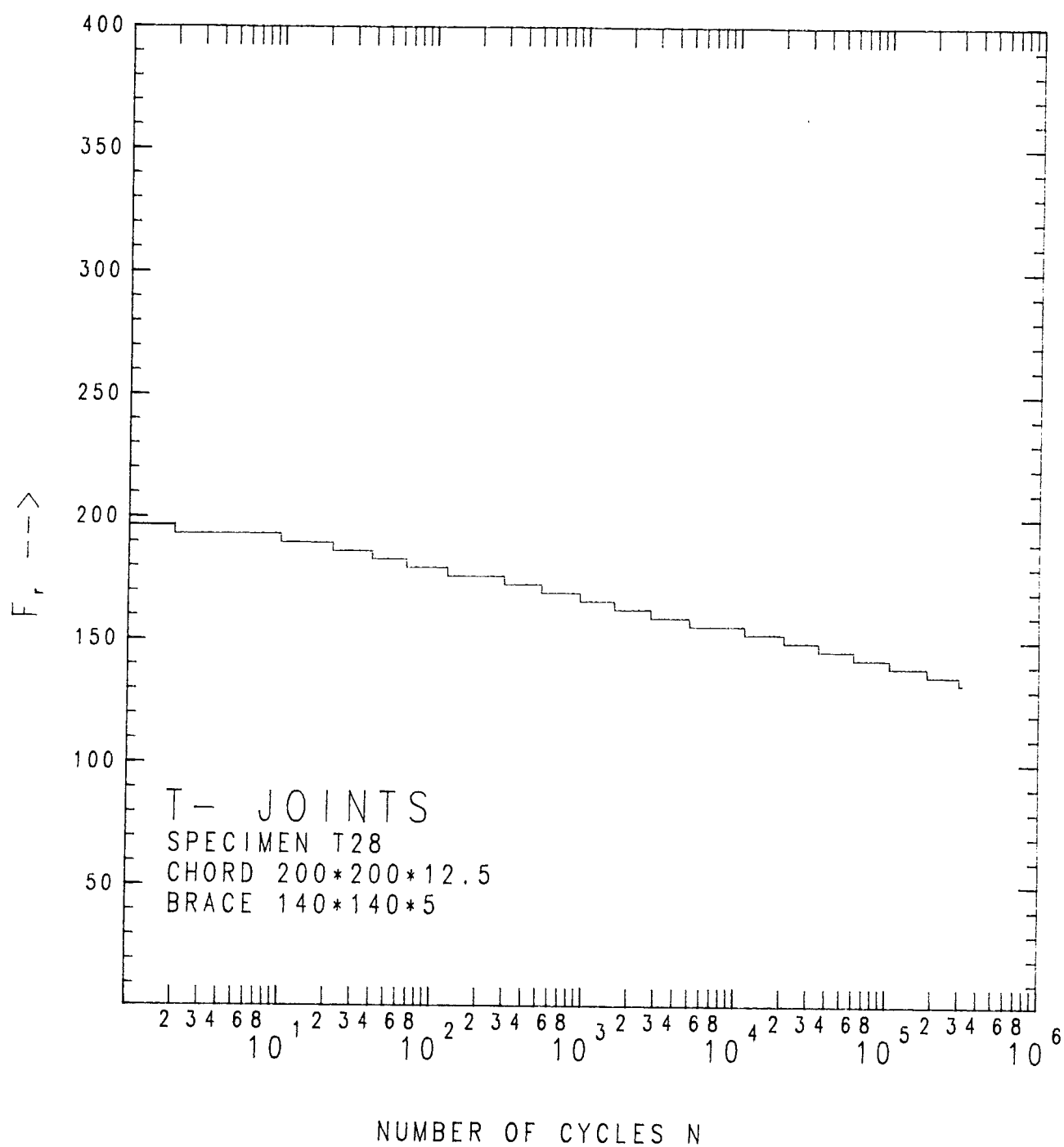


Fig. 25 : Load spectrum for T-joint T28

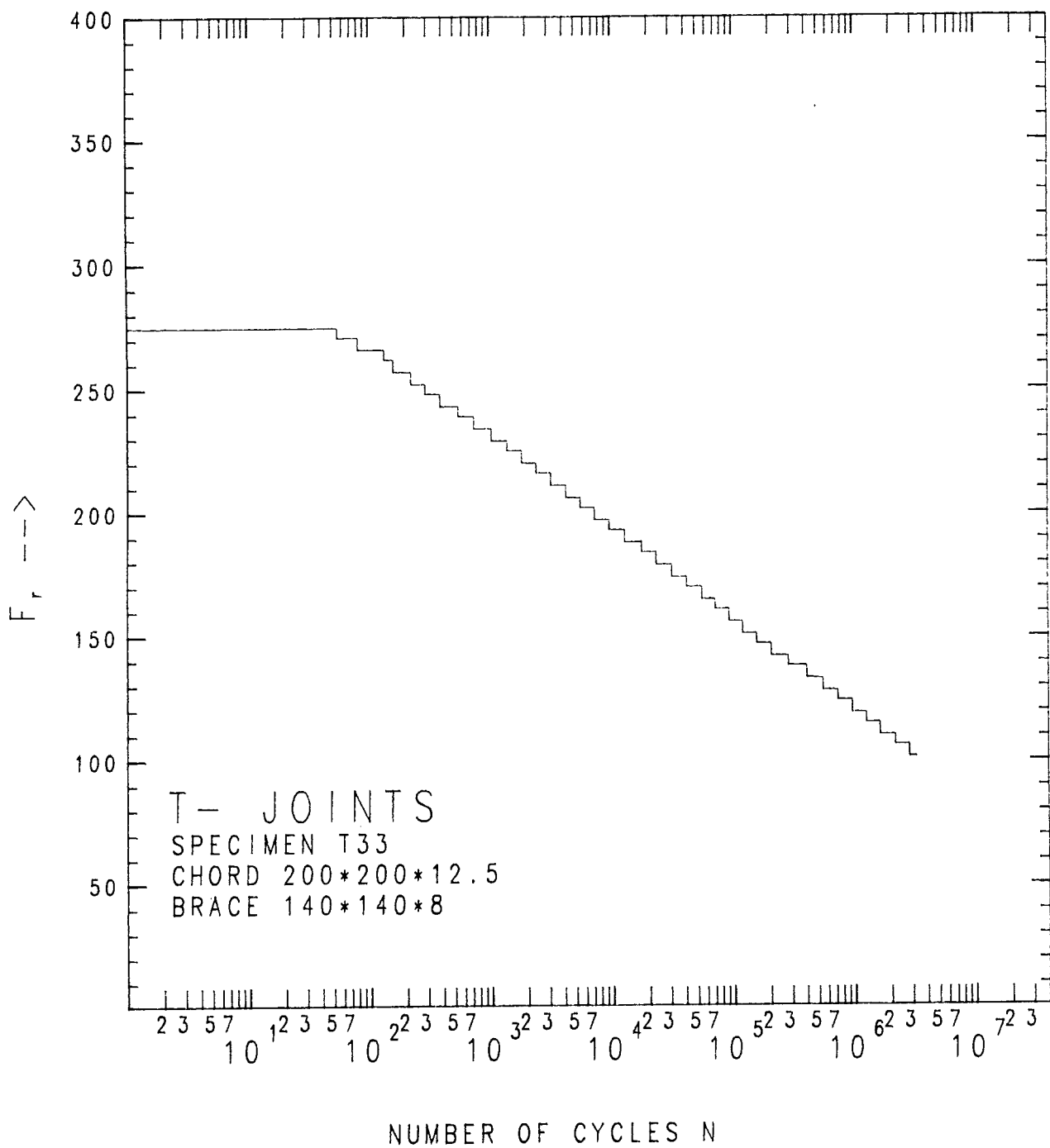


Fig. 26 : Load spectrum for T-joint T33

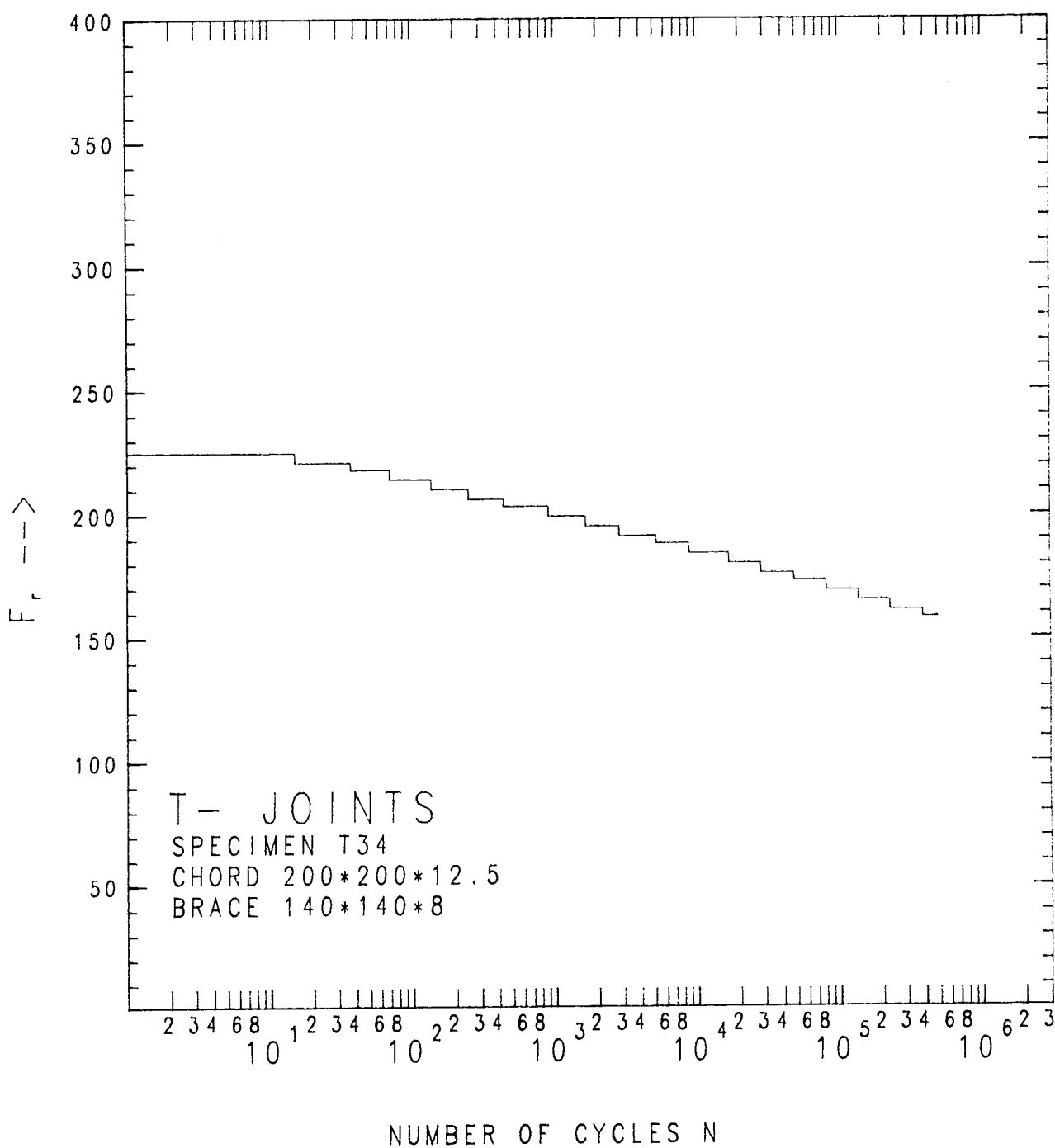


Fig. 27 : Load spectrum for T-joint T34

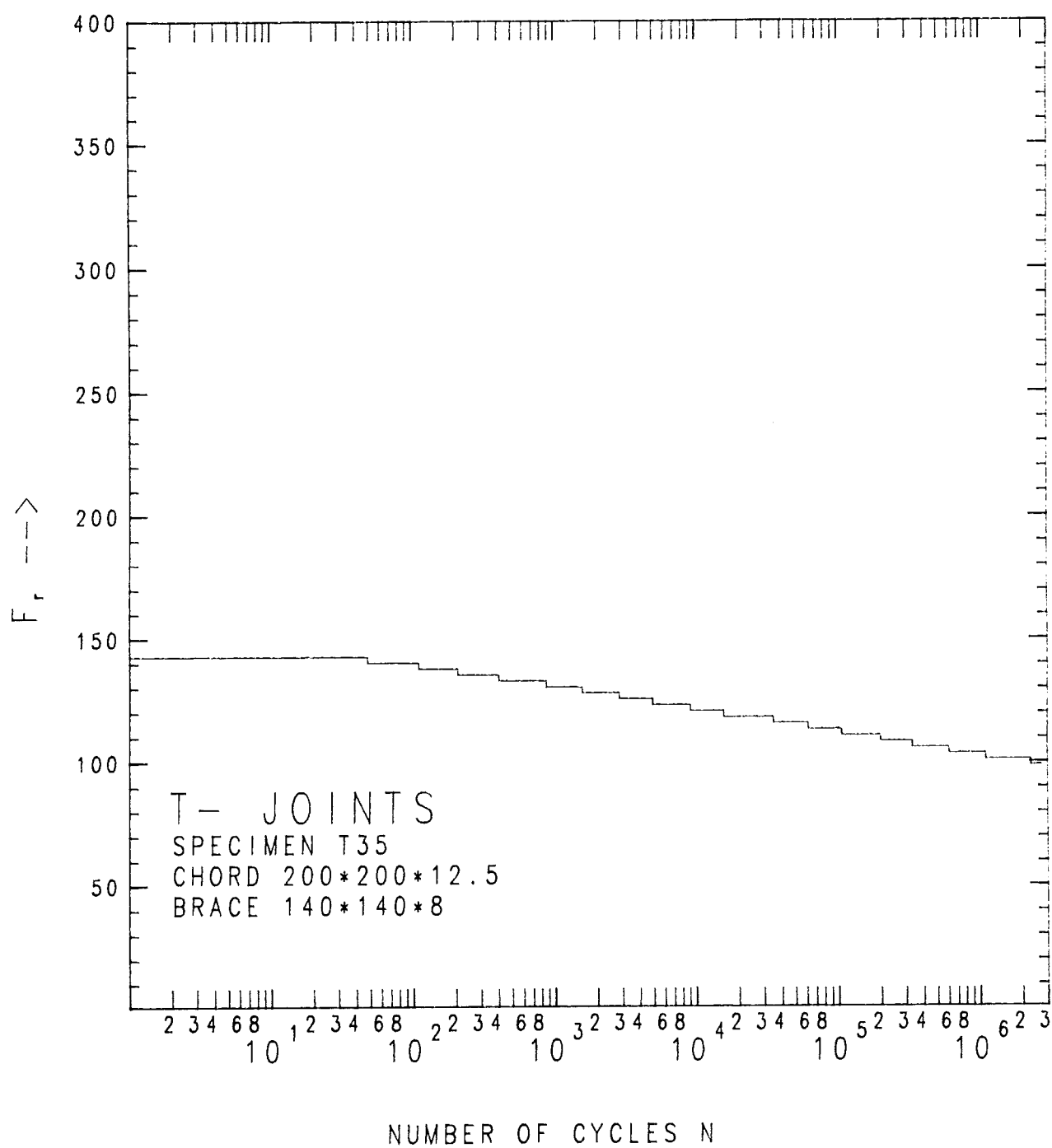


Fig. 28 : Load spectrum for T-joint T35



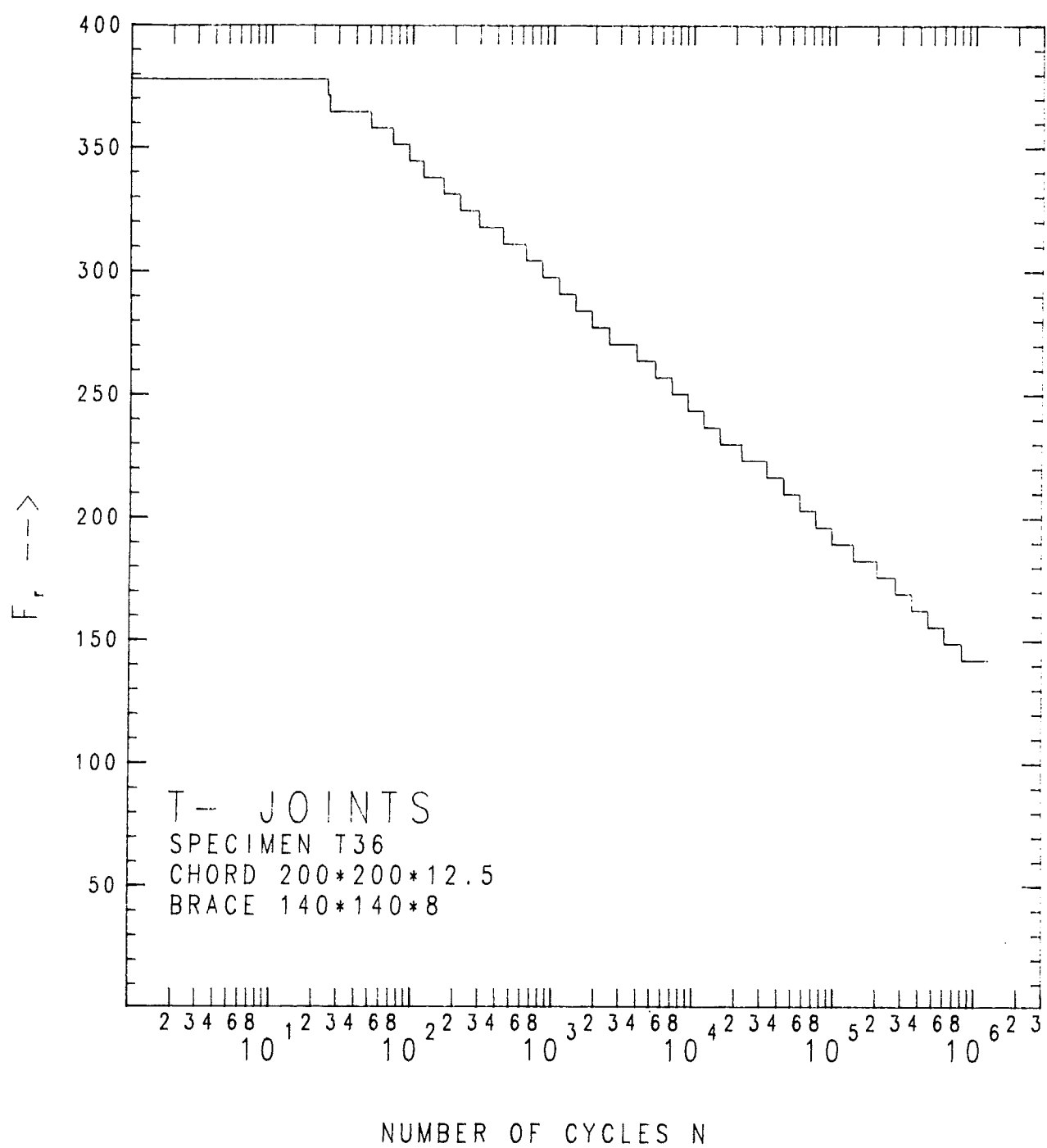


Fig. 29 : Load spectrum for T-joint T36

STRAIN DISTRIBUTION ON THE BRACE AT  $F_{req.} = 122 \text{ kN}$

SPECIMEN T25  
 CHORD : 200\*200\*12.5  
 BRACE : 140\*140\*5

LOC.: GAUGES:  
 O. : 28 TO 31  
 Δ. : 23 TO 26  
 +. : 12 TO 15  
 X. : 7 TO 10

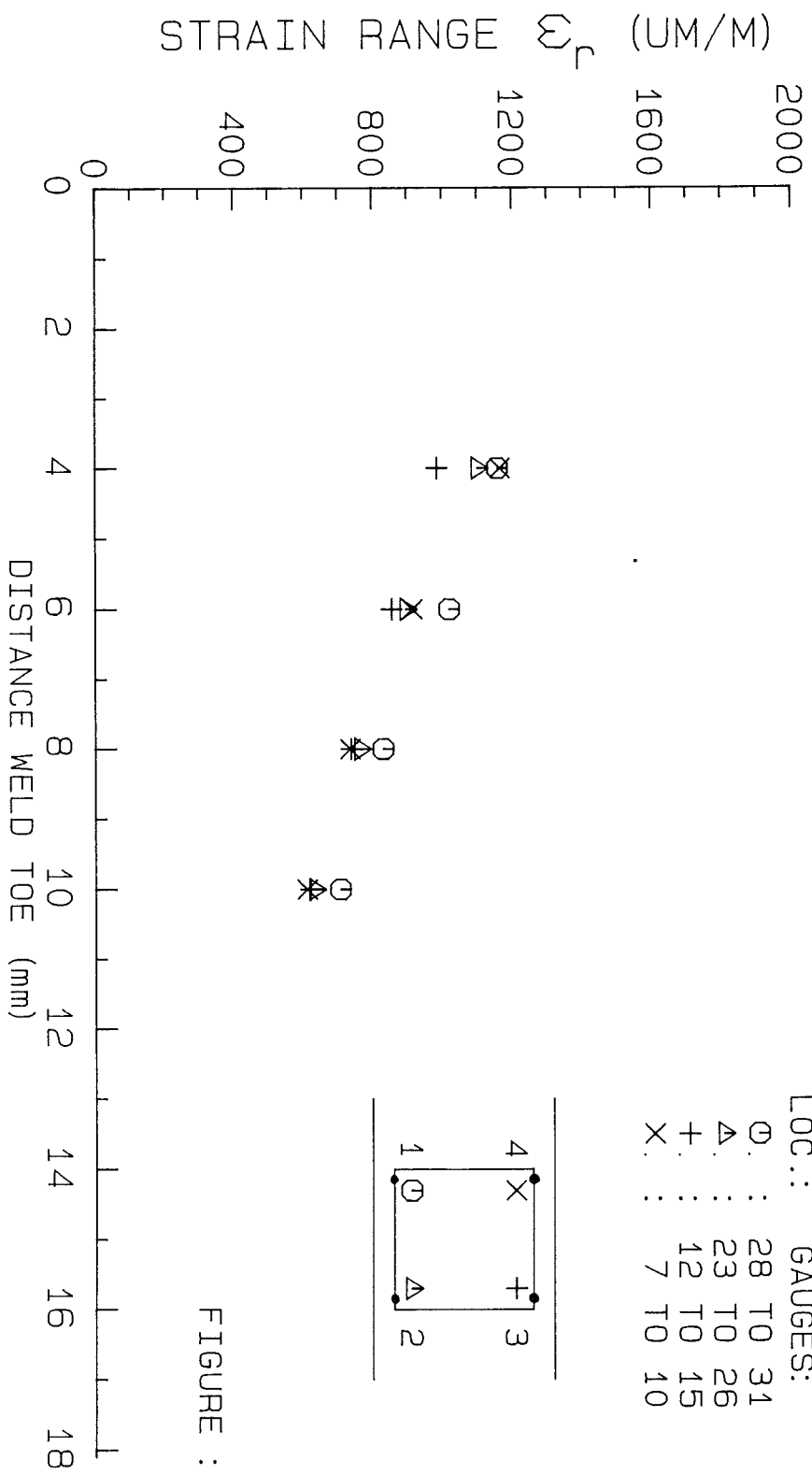
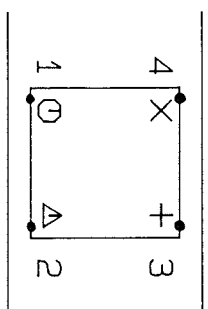


FIGURE : 30

STRAIN DISTRIBUTION ON THE CHORD at  $F_{req.} = 69 \text{ kN}$

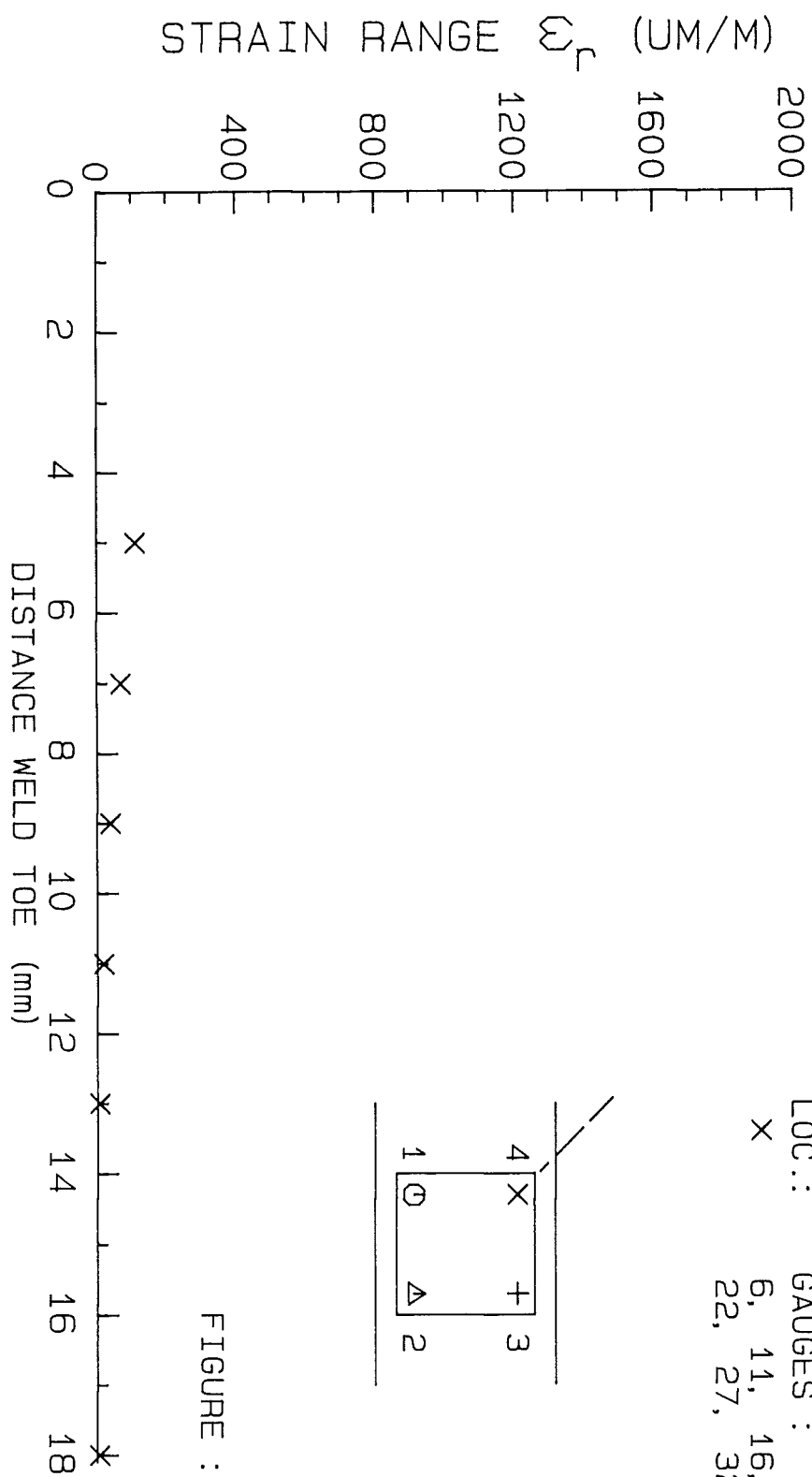
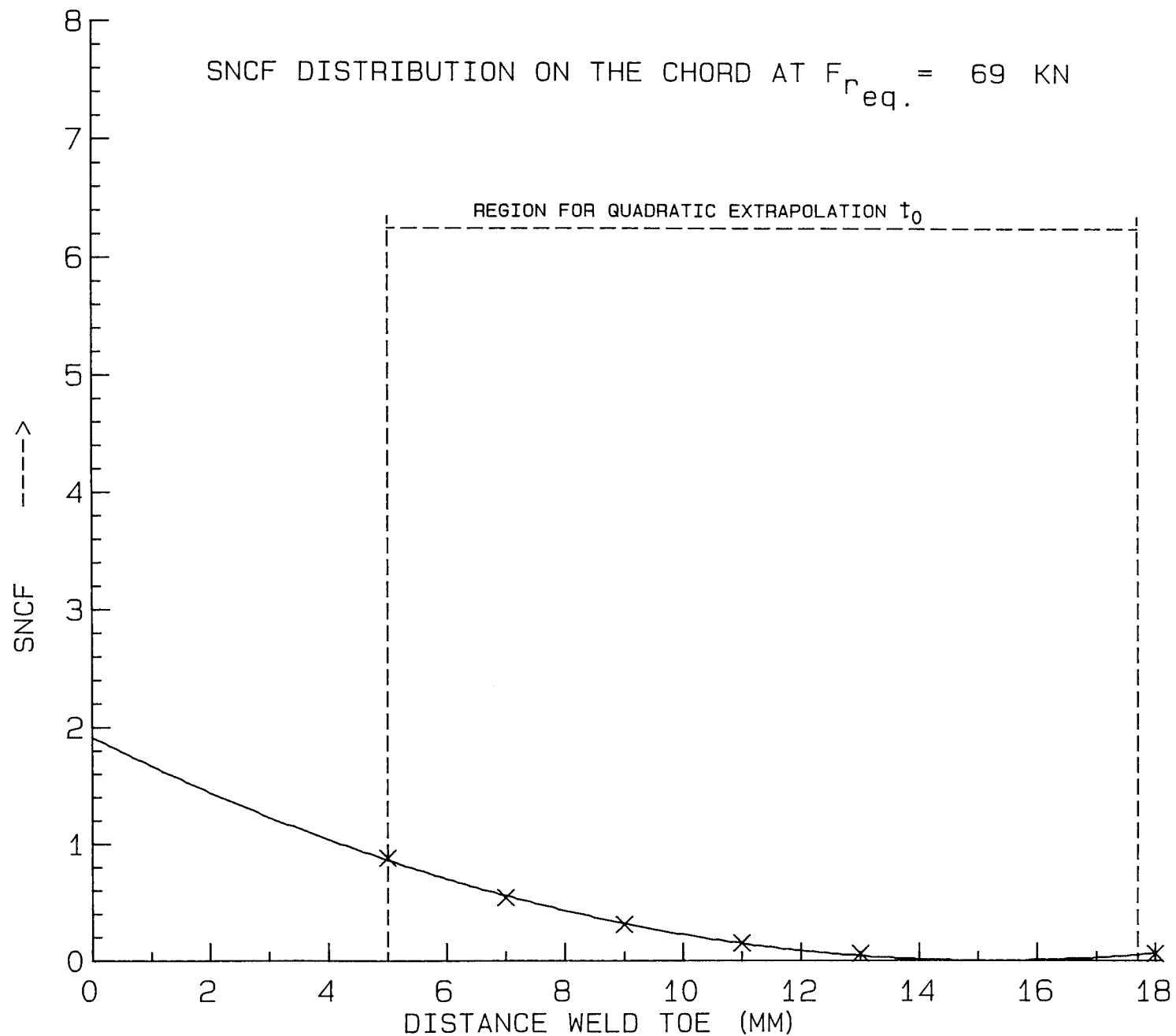


FIGURE : 40



SPECIMEN T27  
 CHORD : 200\*200\*12.5  
 BRACE : 140\*140\*5

LOC.:      GAUGES:  
 ×          6, 11, 16  
             22, 27, 32

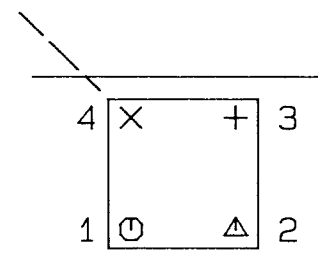
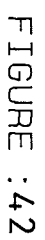


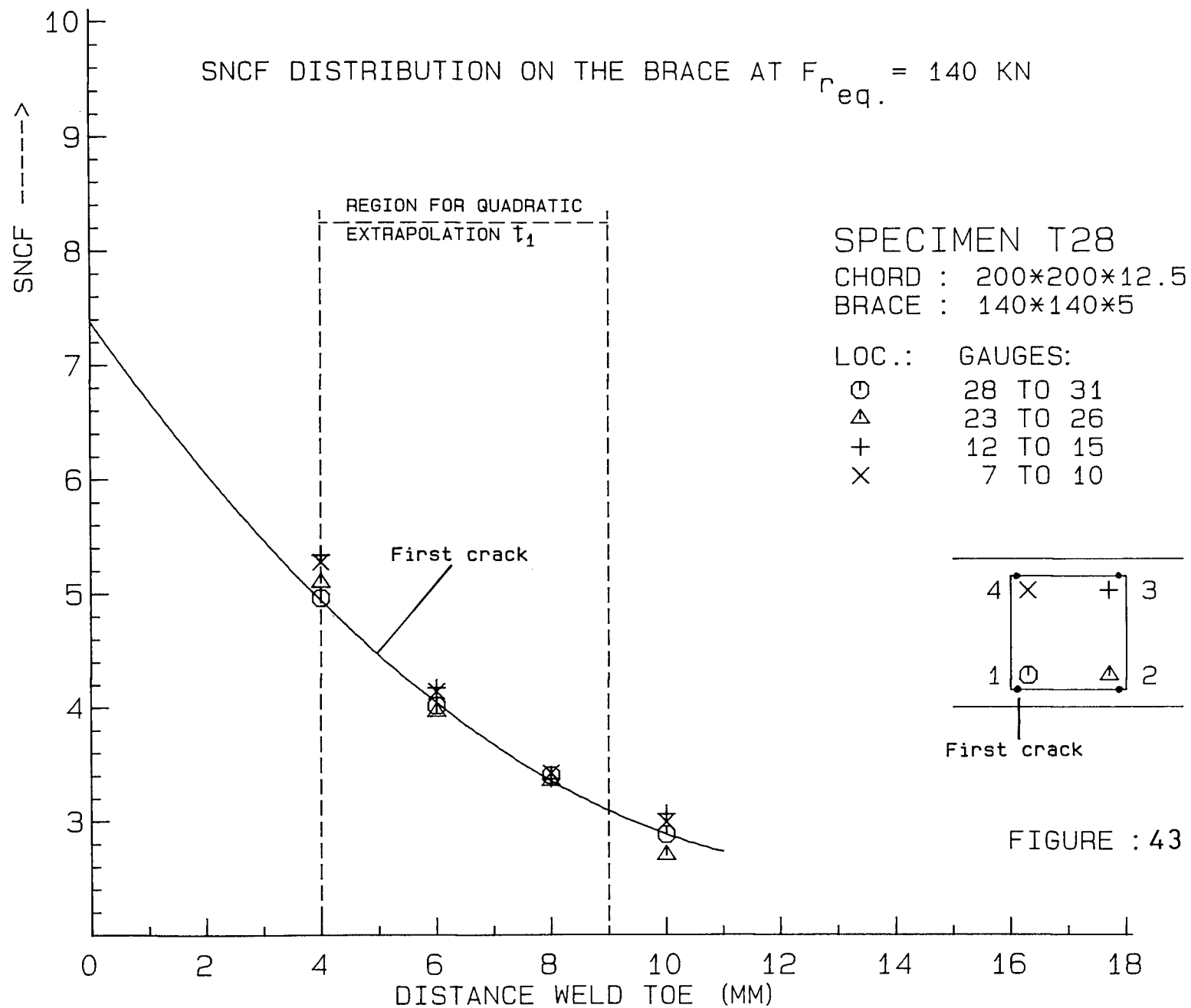
FIGURE :41

$$F_{req.} = 141 \text{ kN}$$

CHORD : 200\*200\*12.5  
BRACE : 140\*140\*5

Symbol	Count	Percentage
0	28	31
1	23	26
2	12	15
3	7	10





STRAIN DISTRIBUTION ON THE CHORD at  $F_{req.} = 141 \text{ kN}$

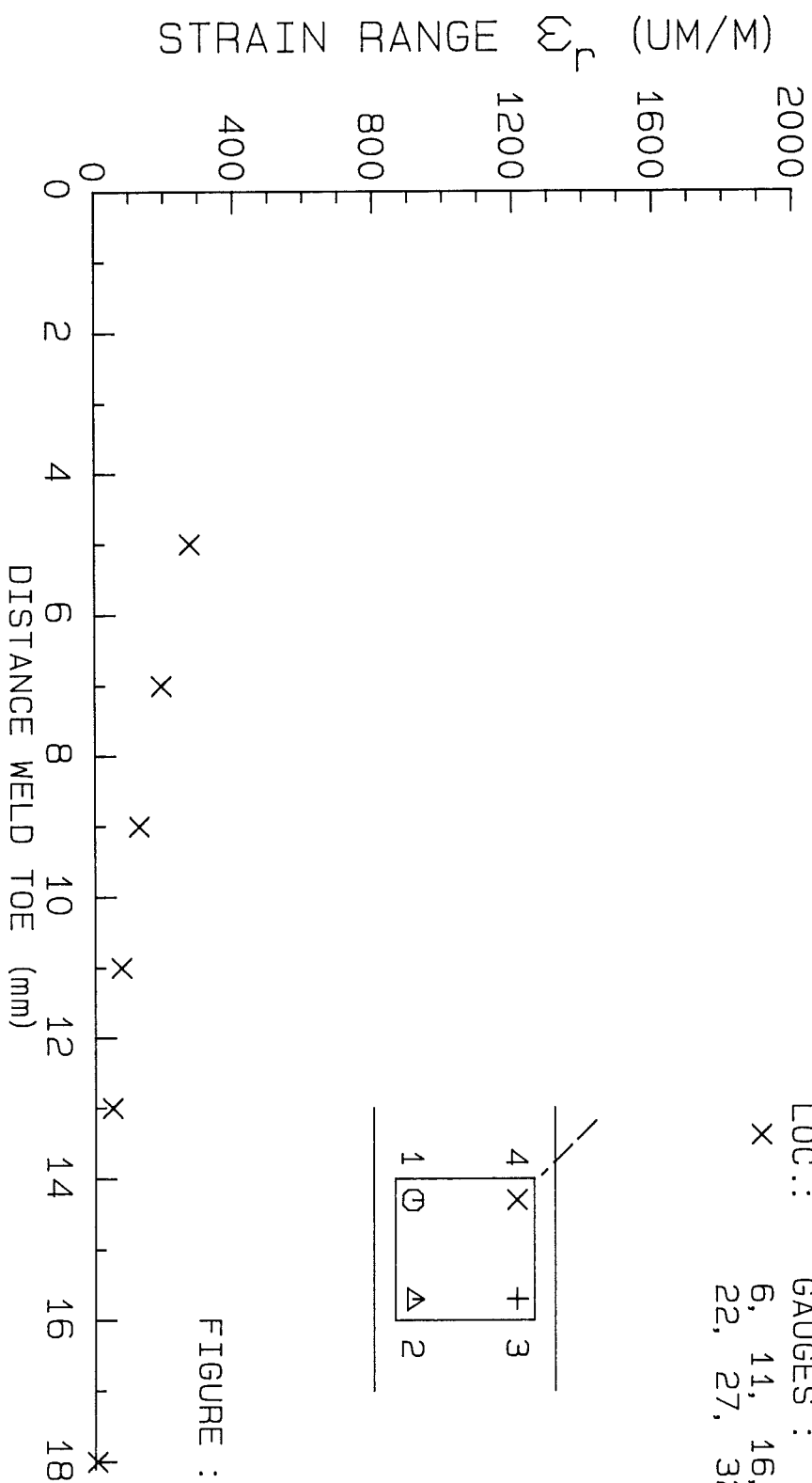


FIGURE : 44

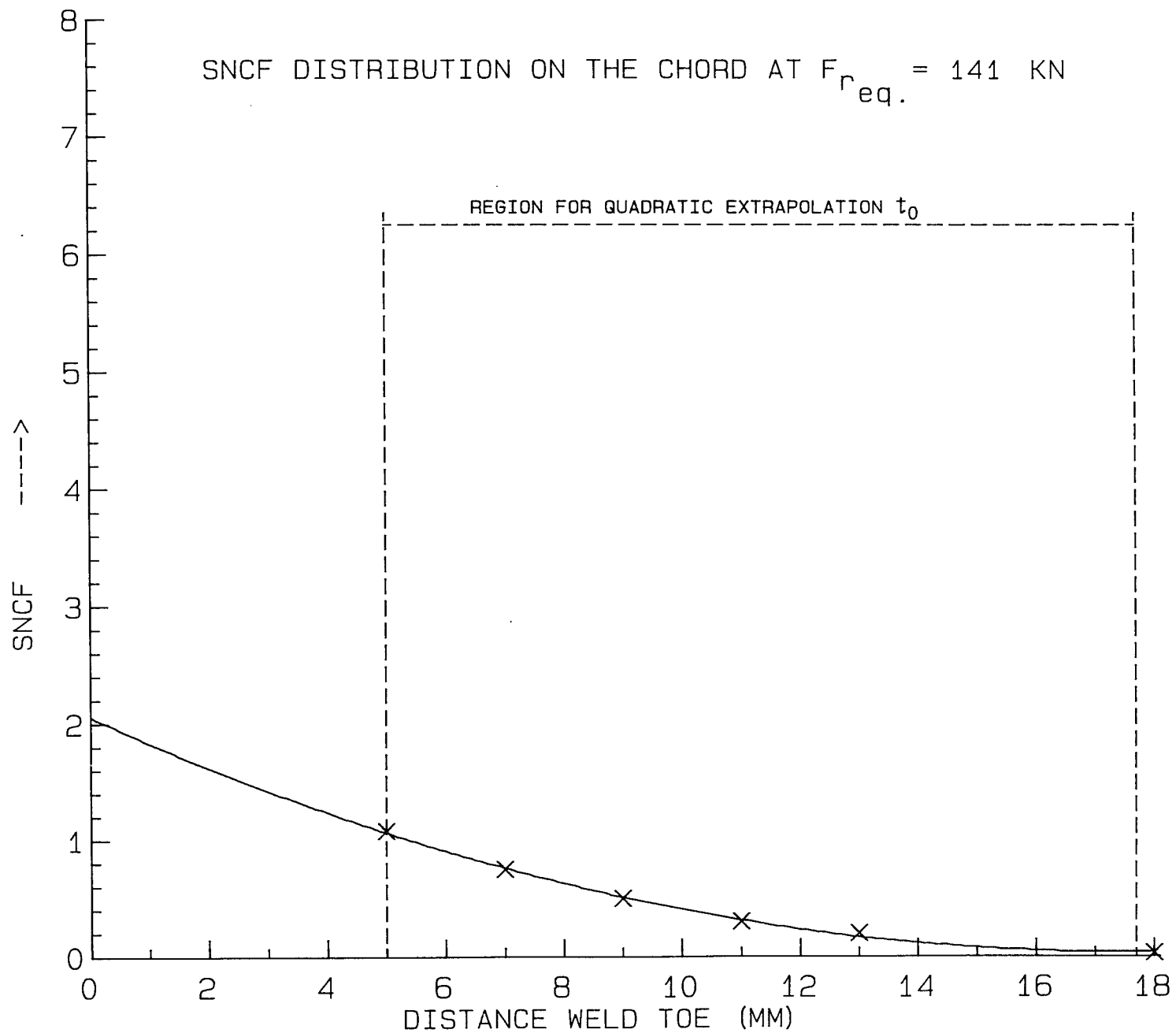
SPECIMEN T28

CHORD : 200\*200\*12.5

BRACE : 140\*140\*5

LOC.: GAUGES :

X  
6, 11, 16,  
22, 27, 32



SPECIMEN T28  
 CHORD : 200\*200\*12.5  
 BRACE : 140\*140\*5

LOC.: GAUGES:  
 X 6, 11, 16  
 22, 27, 32

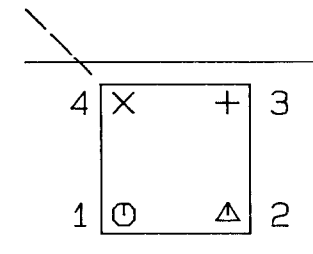


FIGURE : 45



# STRAIN DISTRIBUTION ON THE CHORD AT $F_{req.} = 121 \text{ kN}$

SPECIMEN T33

CHORD : 200\*200\*12.5

BRACE : 140\*140\*8

LOC.: GAUGES:

○.	28 TO 32
△.	23 TO 27
+	12 TO 16
×	7 TO 11

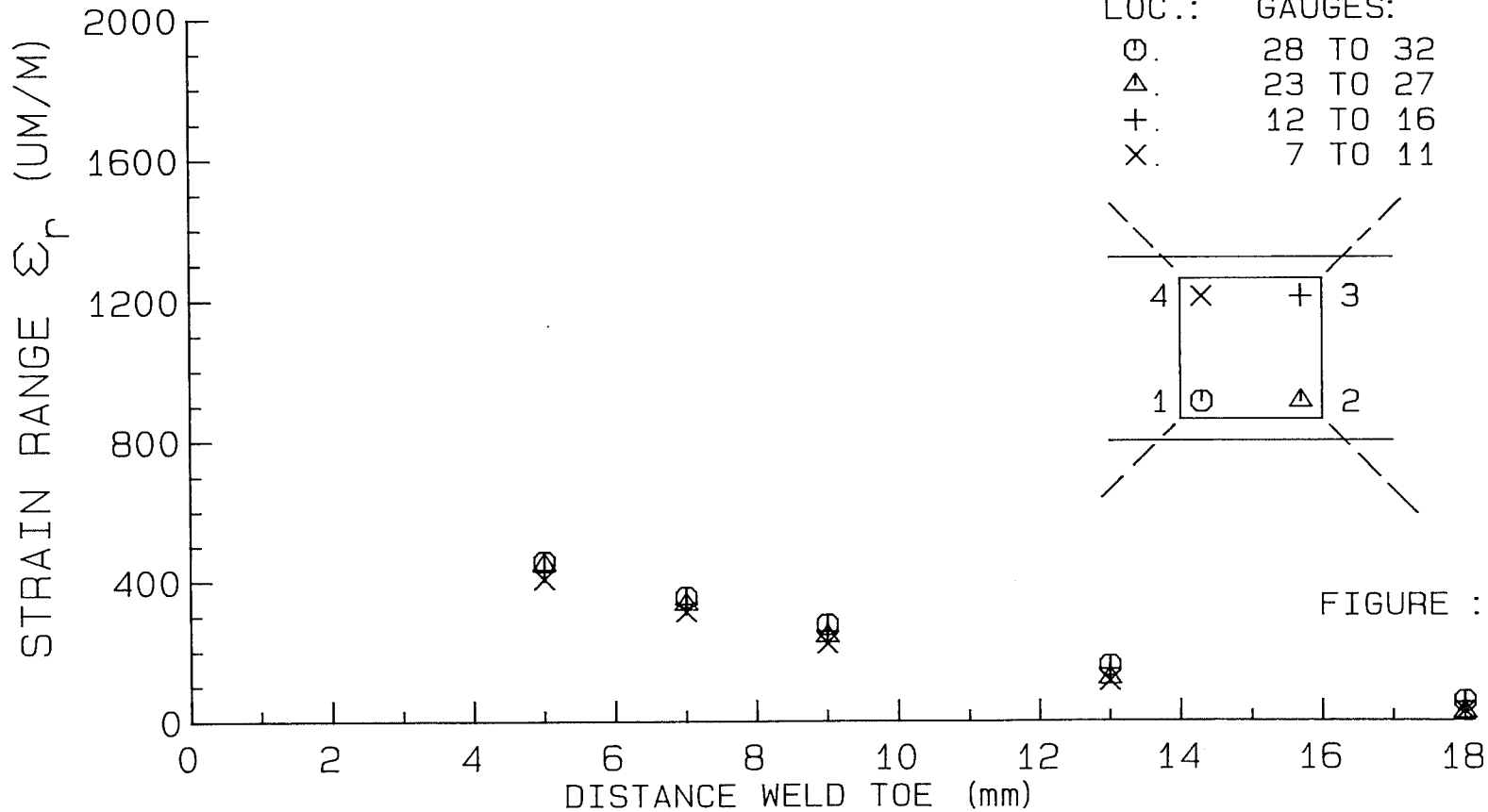
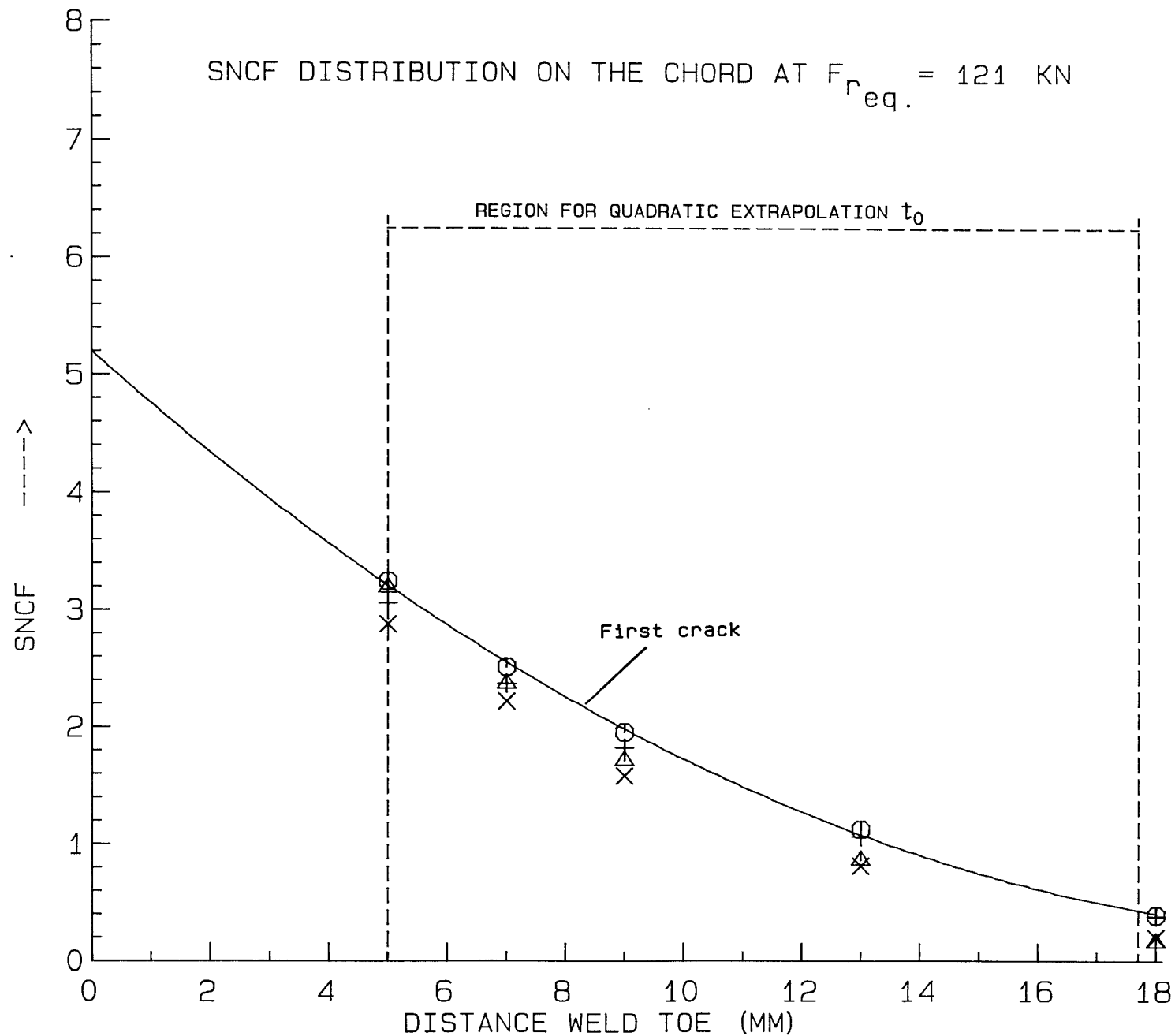


FIGURE : 46



SPECIMEN T33  
 CHORD : 200\*200\*12.5  
 BRACE : 140\*140\*8

LOC.: GAUGES:  
 ○ 28 TO 32  
 △ 23 TO 27  
 + 12 TO 16  
 X 7 TO 11

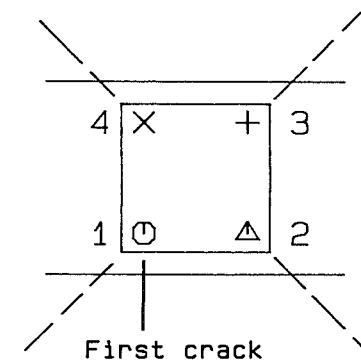
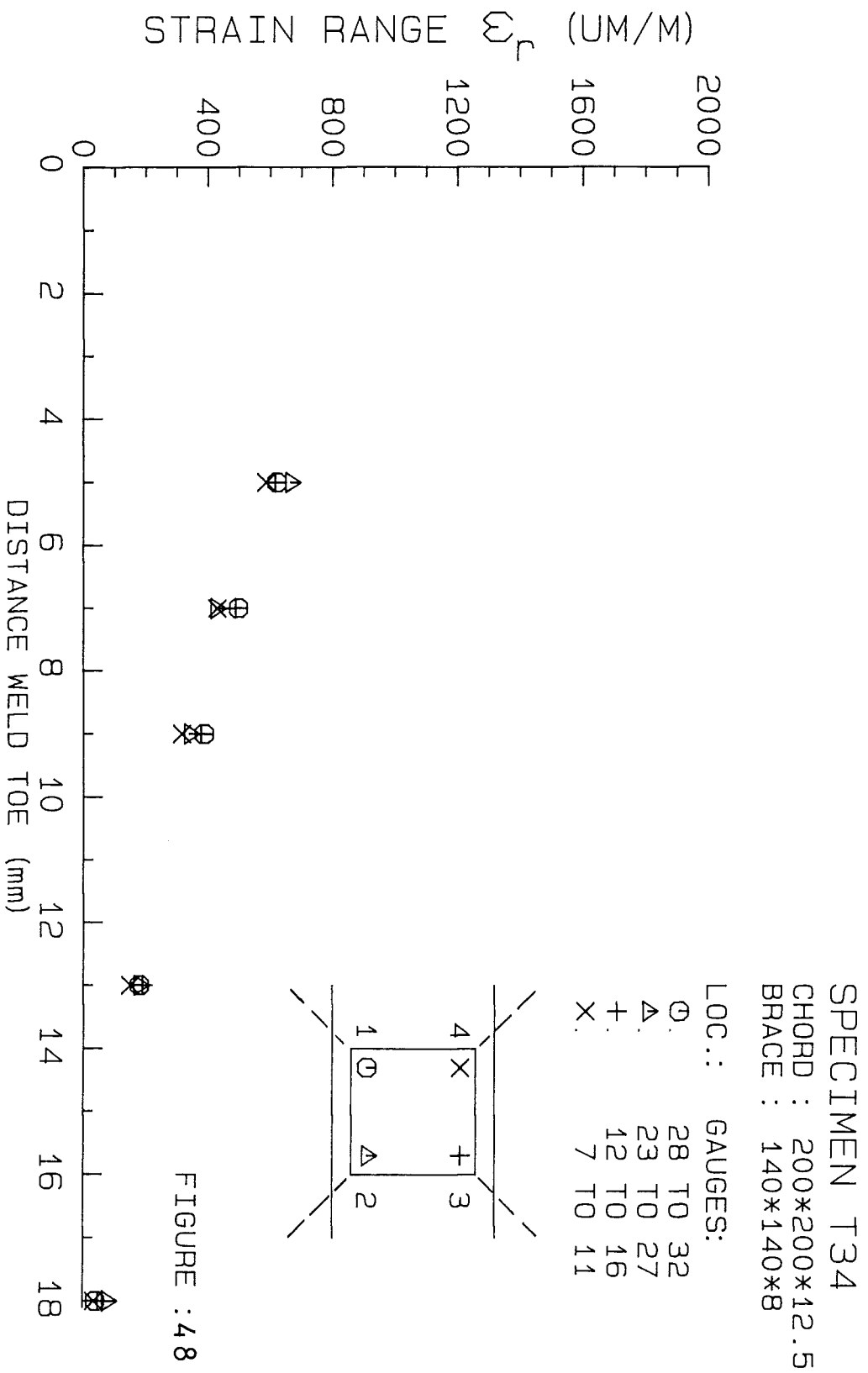
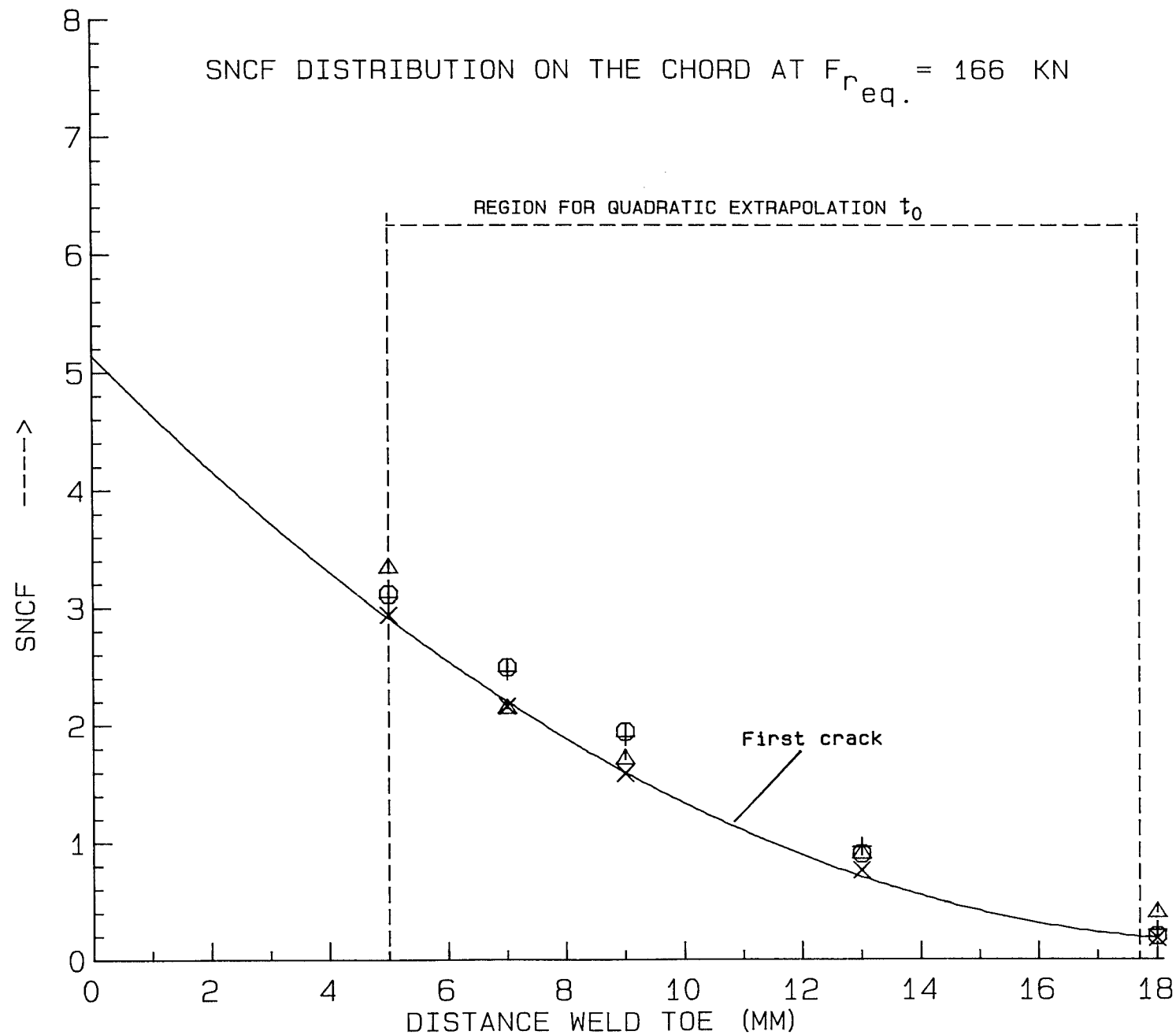


FIGURE :47

STRAIN DISTRIBUTION ON THE CHORD AT  $F_{req.} = 166 \text{ kN}$





SPECIMEN T34  
 CHORD : 200\*200\*12.5  
 BRACE : 140\*140\*8

LOC.:      GAUGES:  
 ○          28 TO 32  
 △          23 TO 27  
 +          12 TO 16  
 ×          7 TO 11

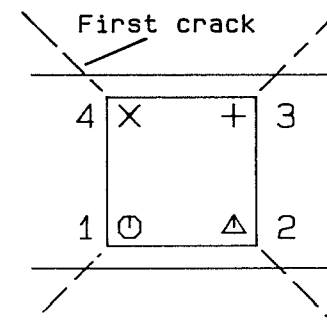
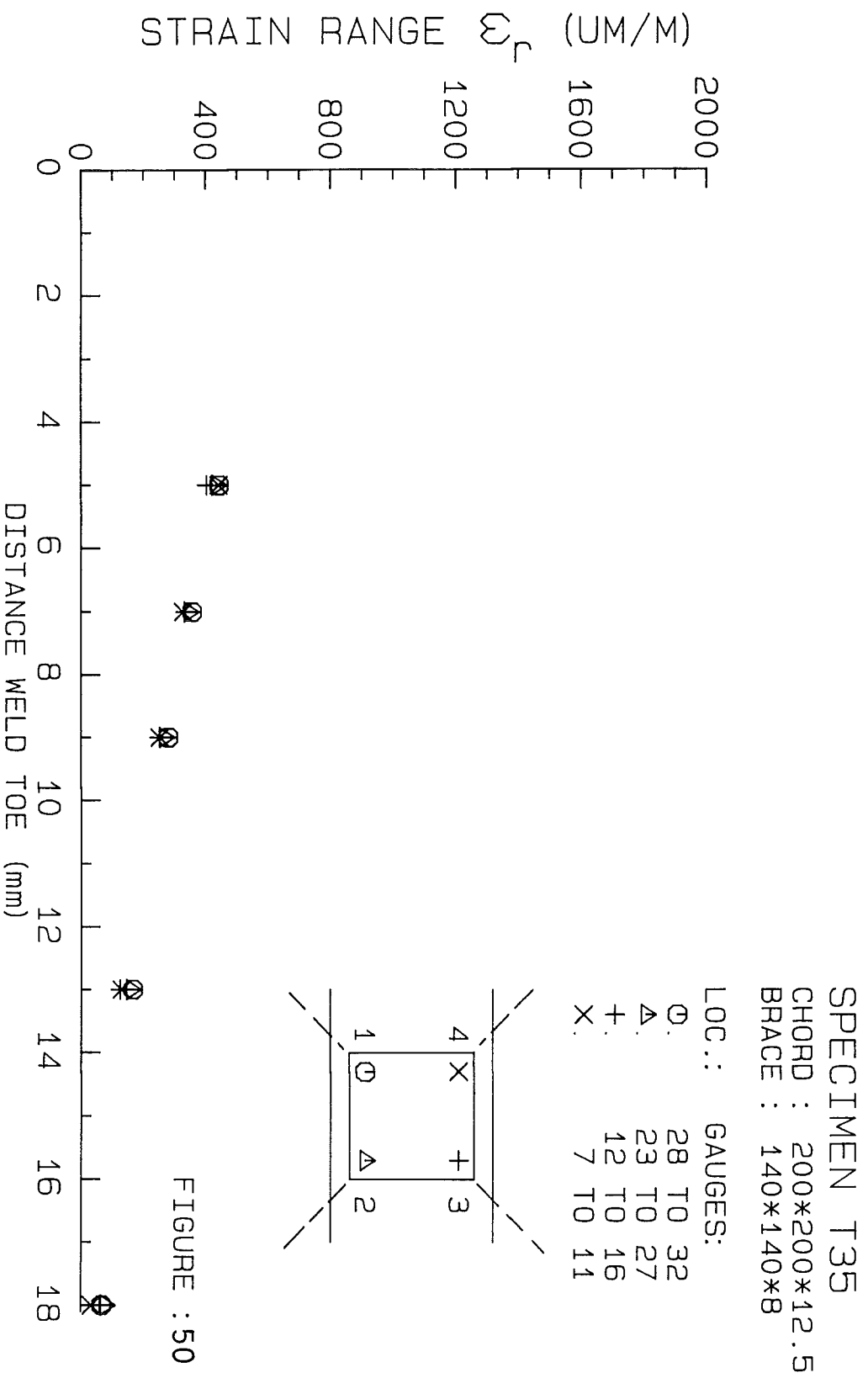
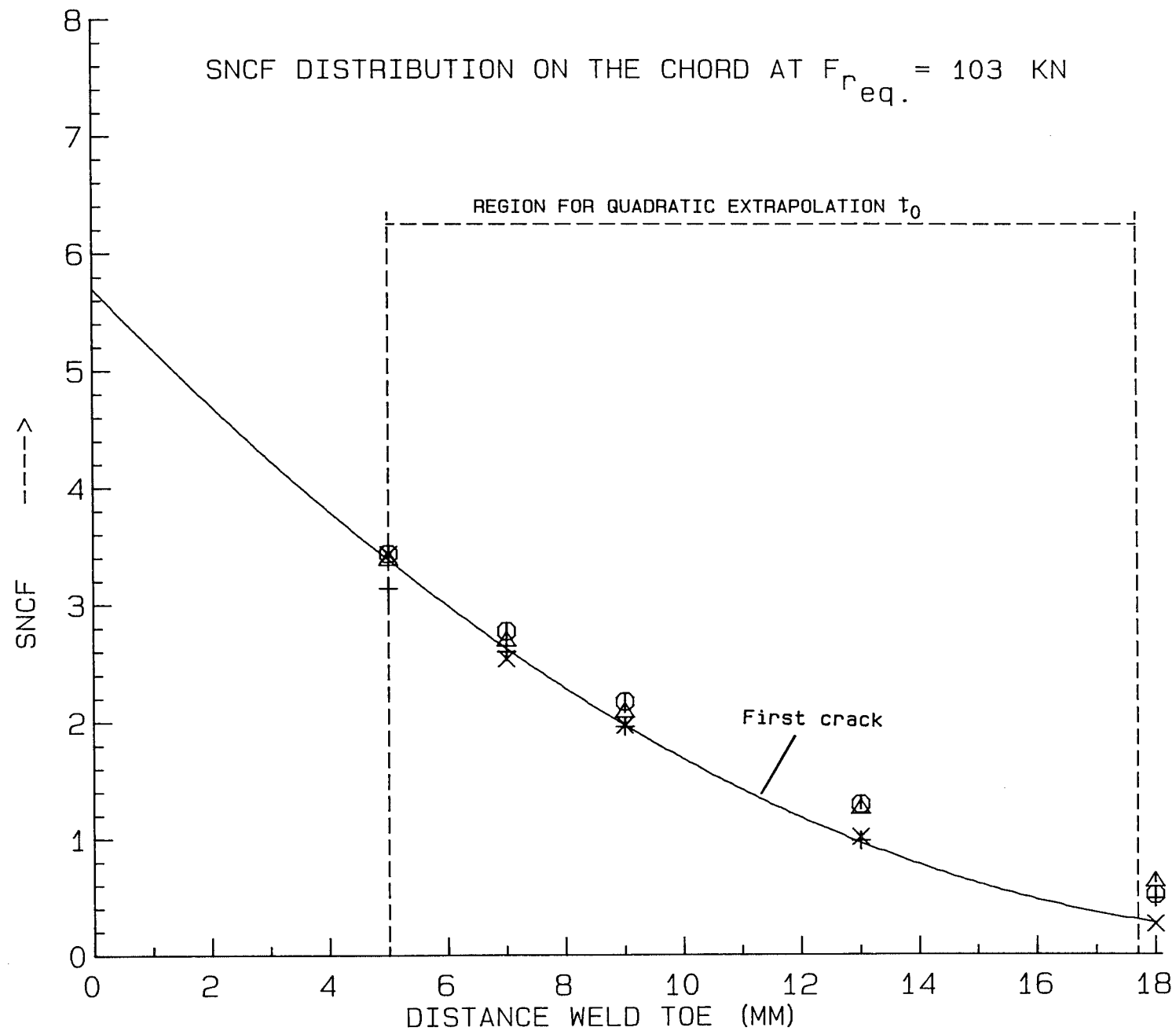


FIGURE : 49

STRAIN DISTRIBUTION ON THE CHORD AT  $F_{req.} = 103 \text{ kN}$





SPECIMEN T35  
 CHORD : 200\*200\*12.5  
 BRACE : 140\*140\*8

LOC.:      GAUGES:  
 ○        28 TO 32  
 △        23 TO 27  
 +        12 TO 16  
 ×        7 TO 11

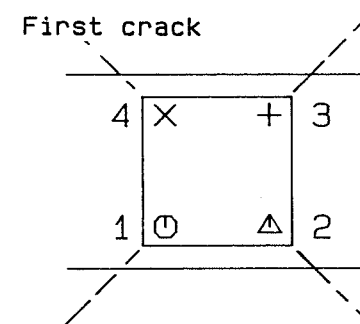


FIGURE : 51

# STRAIN DISTRIBUTION ON THE CHORD AT $F_{req.} = 161 \text{ kN}$

SPECIMEN T36

CHORD : 200\*200\*12.5

BRACE : 140\*140\*8

LOC.: GAUGES:

⊙. 28 TO 32

△. 23 TO 27

+. 12 TO 16

X. 7 TO 11

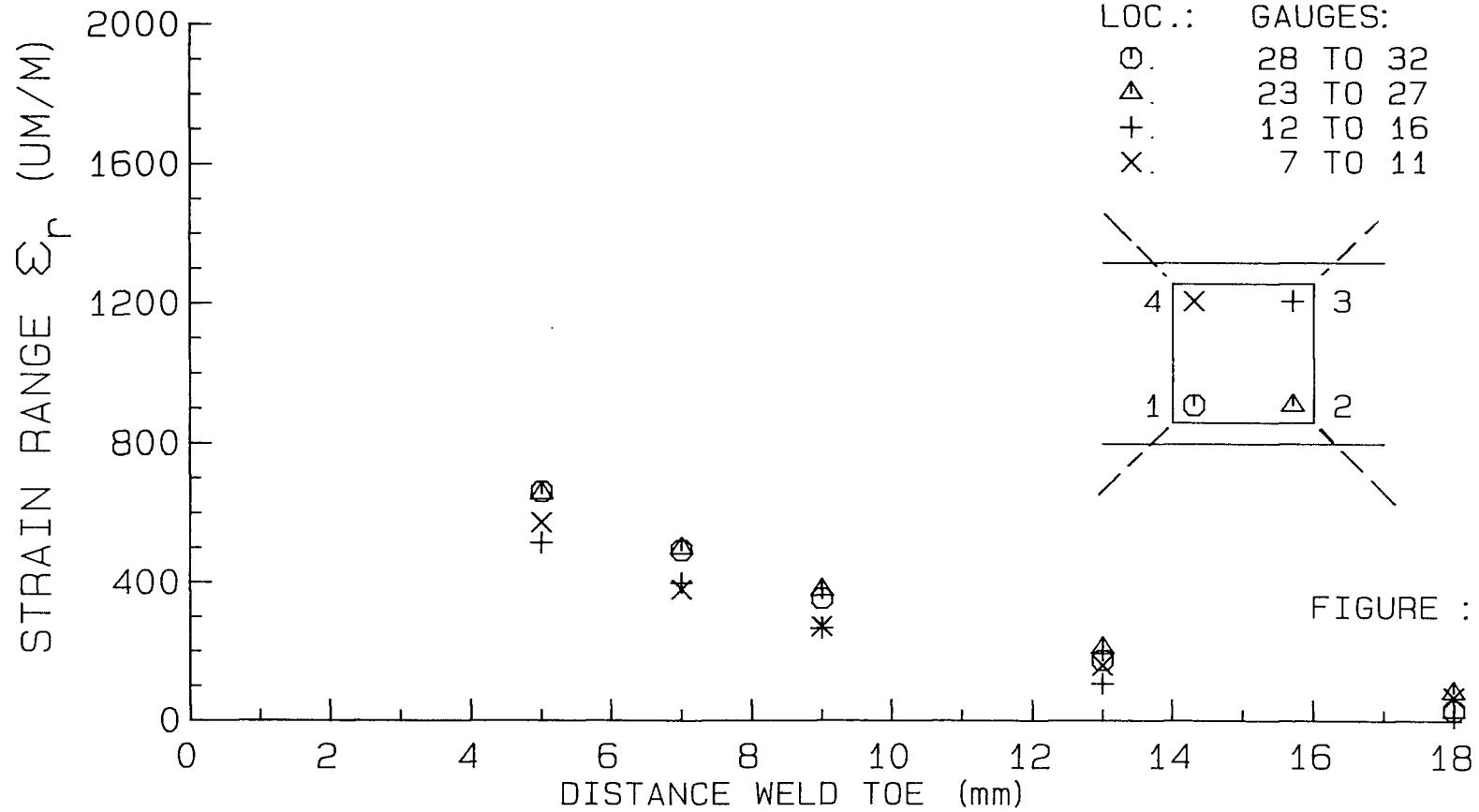
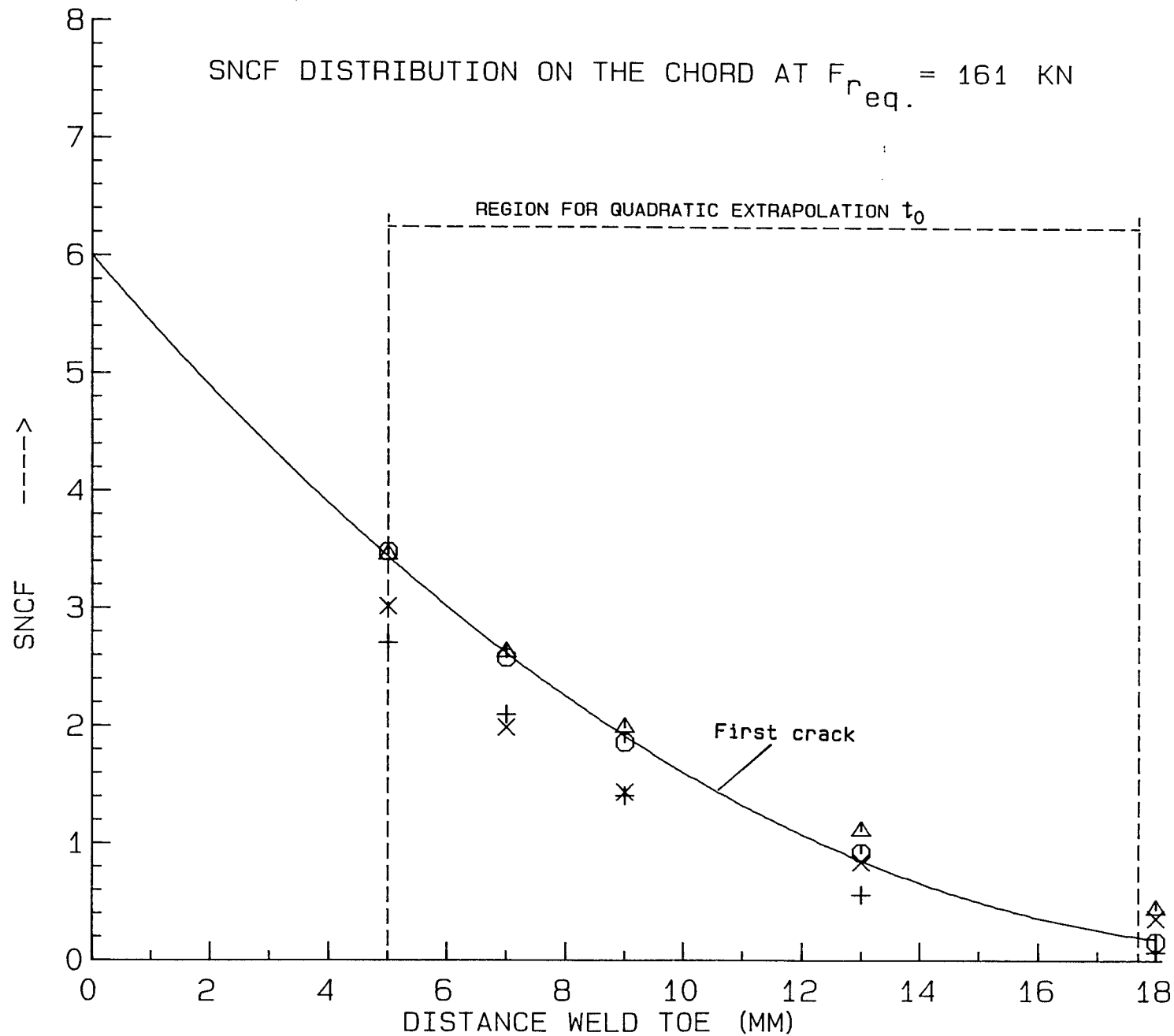


FIGURE : 52



SPECIMEN T36  
 CHORD : 200\*200\*12.5  
 BRACE : 140\*140\*8

LOC.:      GAUGES:  
 ○          28 TO 32  
 △          23 TO 27  
 +          12 TO 16  
 ×          7 TO 11

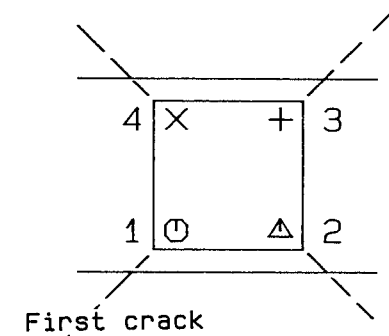


FIGURE : 53